EXPERIMENTAL INVESTIGATION AND NUMERICAL MODELING OF TWO-DIMENSIONAL CHLORIDE DIFFUSION IN CONCRETE

BY

MUHAMMAD UMAR KHAN

A Thesis Presented to the
DEANSHIP OF GRADUATE STUDIES

KING FAHD UNIVERSITY OF PETROLEUM & MINERALS

DHAHRAN, SAUDI ARABIA

In Partial Fulfillment of the
Requirements for the Degree of

MASTER OF SCIENCE

In

CIVIL ENGINEERING

December 2013

KING FAHD UNIVERSITY OF PETROLEUM & MINERALS

DHAHRAN 31261, SAUDI ARABIA

DEANSHIP OF GRADUATE STUDIES

This thesis, written by **MUHAMMAD UMAR KHAN** under the direction of his thesis advisor and approved by his thesis committee, has been presented to and accepted by the Dean of Graduate Studies, in partial fulfillment of the requirements for the degree of **MASTER OF SCIENCE IN CIVIL ENGINEERING**.

Thesis Committee

Dr. Shamshad Ahmad (Advisor)

Dr. Husain Jubran Al-Gahtani (Member)

Dr. Salah U. Al-Dulaijan (Member)

5 MAY 2014

Dr. Nedal T. Ratrout
Departmental Chairman

Dr. Salam A. Zummo
Dean, Graduate Studies

6/5/14

Date

عمادة الدراسات العليا
DEANSHIP OF GRADUATE STUDIES

IN THE NAME OF ALLAH, THE MOST BENEFICIENT, THE MOST MERCIFUL

Dedicated To

My Beloved Parents,

MR. & MRS. ABDUL MALIK KHAN

ACKNOWLEDGEMENTS

All praises and thanks are due to ALLAH (Subhanaho wa taala) for bestowing me with the health, knowledge and patience to complete this work. May the peace and blessings of ALLAH be upon the final Prophet Muhammad (Peace be upon him), his family, and his companions.

I want to thank KFUPM for giving me the opportunity to pursue graduate studies and providing tremendous research facilities and financial assistance during the course of my MS program.

I offer my sincerest gratitude to my Thesis supervisor, Dr. Shamshad Ahmad, who has supported me throughout my work with his patience and knowledge whilst allowing me the room to work in my own way. I would like to acknowledge with eternal gratitude to Prof. Dr. Husain Jubran Al-Gahtani for providing his valuable time and sincere efforts to this research, which has proven to be very interesting and challenging at times. My sincere thanks are extended to my committee member Dr. Salah U. Al-Dulaijan for his valuable comments and suggestions. I am also indebted to the Department Chairman, Dr. Nedal T. Ratrout, and other faculty members for their support.

I have to thank Dr. Mohammad Maslehuddin for extending his support in the experimental work and for his kind advices. I acknowledge grateful thanks to Prof. Dr. Muhammed Baluch for developing the analytical skills and research attitude in myself. My heart full thanks are extended to Engr. M. Mukarram Khan, Engr. Syed Imran Ali, Engr. Mohammed Shameem, Engr. Mohammed Ibrahim, Engr. Mohammed Salihu Barry and Engr. Mohammed Rizwan Ali for their support during this research.

I would like to take this opportunity to thank Mr. Saad, Mr. Nasir and Mr. Waleed for helping me in my experimental program and boosting my confidence. I cannot end without thanking the friendly and cheerful group of fellow students, who helped and stood by me during the course of my stay at the University. I would also like to thank any others whom I may have missed, who have, directly or indirectly, contributed to my research.

My parents and family deserve special acknowledgement for encouraging me to pursue my degree. I have relied on their love and support throughout all my academics. Their unflinching courage and conviction always inspired me and without their patience and prayers this modest contribution to Civil Engineering could not have been made.

TABLE OF CONTENTS

LIST OF TABLES

LIST OF FIGURES

LIST OF NOTATIONS

f_c'	Compressive strength in MPa
w/c	Water to cement ratio
w/cm	Water to cementitious material ratio
t	Exposure duration in days
D	Chloride diffusion coefficient in cm^2/sec
C_s	Surface chloride concentration
IC	Initial condition
BC	Boundary condition
k	Chloride binding factor
^oC	Degree Celsius

ABSTRACT (ENGLISH)

NAME: **MUHAMMAD UMAR KHAN**

TITLE: **EXPERIMENTAL INVESTIGATION AND NUMERICAL MODELING OF TWO-DIMENSIONAL CHLORIDE DIFFUSION IN CONCRETE**

MAJOR: **CIVIL ENGINEERING**

DATE: **DECEMBER 2013**

Chloride diffusivity is an essential attribute of concrete. Durability of reinforced concrete structures subjected to chloride exposures are affected by it. The time of initiation of chloride-induced reinforcement corrosion mainly depends on chloride diffusion coefficient and cover thickness. Surface concrete having lower chloride diffusion coefficient and higher cover thickness is required to enhance the service life of reinforced concrete structures against reinforcement corrosion. Chloride diffusion coefficient of concrete is therefore one of the key parameters needed for prediction of initiation of reinforcement corrosion which is required for durable design of new concrete structures and for taking decisions regarding protection of existing reinforced concrete structures under severe chloride exposure conditions.

Fick's 2nd law of diffusion has been used for long time to derive the models for chloride diffusion in concrete. However, such models do not include the effects of various significant factors such as chloride binding by the cement, multi-directional ingress of chloride, and variation of chloride diffusion coefficient with time due to change in the microstructure of concrete during early period of cement hydration. Therefore, it is required to develop a model that would consider the effect of chloride binding, 2-D ingress of chloride in concrete and change in the microstructure with time.

The chloride diffusion model developed considering the effect of these factors, relevant to concrete, would enable in predicting the service life of reinforced concrete structures more accurately.

In the proposed work, first an experimental program was conducted to generate data for obtaining chloride profiles (i.e., the variation of chloride content along the depth of concrete) at different exposure durations. Then, based on the review of different models as reported in literature, a new model was proposed for determination of chloride diffusion coefficient with the provision of incorporating the effects of the time and chloride binding. The proposed model (i.e., differential equation representing the chloride diffusion process) can be solved using numerical analysis for calculation of chloride diffusion coefficient, surface chloride concentration and chloride binding coefficient. The same model can be utilized in predicting the time of initiation of reinforcement corrosion by substituting the calculated values of chloride diffusion coefficient, surface chloride concentration and chloride binding coefficient into the proposed model corresponding to cover depth and threshold chloride concentration. By comparing the results obtained using different models including the proposed one, the effects of time and chloride binding on diffusion coefficient and corrosion initiation time was observed.

ملخص الرسالة

الاسم: محمـــد عمـــر خـــان

العنوان: التحقيق التجريبي والنمذجة العددية لنفاذية الكلوريد ثنائي الأبعاد في الخرسانة

الرئيسية: الهندسة المدنية

التاريخ: ديسمبر 2013

يعتبر نفاذية الكلوريد هو سمة أساسية في الخرسانة. تتأثر متانة المنشآت الخرسانة المسلحة المعرضة لمخاطر الكلوريد به. وقت بدء التأكل في التسليح بسبب الكلوريد يعتمد أساسا على معامل نفاذية الكلوريد وسمك الغطاء. تحسين عمر الخدمة للمنشآت الخرسانية ضد تأكل حديد التسليح يتطلب معامل نفاذية منخفض للكلوريد وزيادة سماكة الغطاء الخرساني. لذا معامل نفاذية الكلوريد في الخرسانة هو واحدة من المعايير الأساسية المطلوبة للتنبؤ ببدء تآكل الخرسانة وهو مطلوب لتصميم المنشآت الخرسانية المعمرة الجديدة واتخاذ قرارات بشأن حماية المنشآت الخرسانية المسلحة الموجودة تحت ظروف التعرض القاسية للكلوريد.

وقد استخدم القانون (Fick's 2^{nd}) للنفاذية لفترة طويلة لاشتقاق نماذج نفاذية الكلوريد في الخرسانة. ومع ذلك، مثل هذه النماذج لا تشمل تأثيرات العوامل المختلفة الهامة مثل استيعاب الكلوريد من قبل الاسمنت. تسرب الكلوريد في اتجاهات متعددة ، والاختلاف معامل نفاذية الكلوريد مع مرور الوقت بسبب تغيير في البنية المجهرية من الخرسانة أثناء الفترة المبكرة من اماهة الإسمنت. لذلك، هو مطلوب تطوير نموذج من شأنه أن ينظر في تأثير استيعاب الكلوريد ، نفاذية الكلوريد في الخرسانة في اتجاهين والتغيير في البنية المجهرية مع مرور الوقت. تطوير نموذج لنفاذية الكلوريد يأخذ بنظر الاعتبار تأثير هذه العوامل، ذات الصلة بالخرسانة، سيمكن في التنبؤ خدمة الحياة للمنشآت الخرسانة المسلحة بشكل أكثر دقة.

في العمل المقترح، وأجريت أول برنامج تجريبي لتوليد بيانات للحصول على مقطع جانبي للكلوريد (بمعنى اختلاف محتوى الكلوريد على طول عمق الخرسانة) لفترات تعرض مختلفة. ثم، استنادا إلى استعراض نماذج مختلفة كما ورد في المؤلفات، اقترح نموذجا جديدا لتحديد معامل نفاذية الكلوريد و

يتضمن الاثار المترتبة على الوقت و استيعاب الكلوريد. النموذج المقترح (أي المعادلة التفاضلية التي تمثل عملية نفاذية الكلوريد) يمكن حلها باستخدام التحليل العددي لحساب معامل نفاذية الكلوريد، تركيز الكلوريد السطحي ومعامل استيعاب الكلوريد. ويمكن استخدام نفس النموذج في توقع وقت بدء تآكل التسليح عن طريق استبدال القيم المحسوبة لمعامل نفاذية الكلوريد، تركيز الكلوريد السطحي ومعامل استيعاب الكلوريد في النموذج المقترح المقابلة لعمق الغطاء وحدود تركيز الكلوريد. من خلال مقارنة النتائج التي تم الحصول عليها باستخدام نماذج مختلفة بما في ذلك النموذج المقترح، لوحظ تأثير الزمن و استيعاب الكلوريد على معامل النفاذية و وقت بدء التآكل.

درجة الماجستير في العلوم الهندسية
جامعة الملك فهد للبترول والمعادن
الظهران – ٣١٢٦١
المملكة العربية السعودية

CHAPTER 1

INTRODUCTION

1.1 Introduction

Deterioration of reinforced concrete structures due to chloride-induced reinforcement corrosion has been reported to be a major durability problem worldwide. In Arabian Gulf region, the climate is characterized by high temperature and humidity and there are large fluctuations in the diurnal and seasonal temperature and humidity. The temperature can vary by as much as 20 ºC during a summer day and the relative humidity ranges from 40-100% over 24 hours. These sudden and continuous variations in temperature and humidity initiate cycles of expansion / contraction and hydration / dehydration, which results in the cracking and durability problems in concrete [1]. During several decades, a large number of infrastructures have been constructed by concrete. It is estimated that at present, about 2 billion tons of reinforced concrete is being built every year [2]. However, the deterioration of reinforced concrete constructed infrastructures directly affects on everyday life in terms of safety and economy. A significant fraction of concrete produced is increasingly being used for repair and rehabilitation rather than new construction and it poses an economic burden on the society [3].

Chloride induced reinforcing steel corrosion is one of the most important and common material deterioration problems in reinforced concrete structures. A large number of infrastructures are affected by it, particularly those which are exposed to coastal / marine conditions. In order to protect the reinforcing steel from corrosion, one

has to understand the mechanism of chloride penetration in concrete and the factors influencing it [4].

Unlike the other porous mediums, the penetration of chloride ions in concrete is a complex non-linear dynamic phenomenon including several transport mechanisms (ionic diffusion, capillary sorption, permeation, dispersion, etc.) [5–7]. The ionic diffusion is considered to have the most dominant effect under the assumption that concrete cover is fully saturated [8]. In saturated state, the chloride ions enter the concrete by ionic diffusion due to the concentration gradient between the exposed surface and the pore solution of concrete. This process is often described by Fick's 2^{nd} law of diffusion. Crank gave the solution of this governing partial differential equation with semi-infinite boundary conditions and assumed diffusion coefficient as constant [9]. However, various researchers have reported that diffusion coefficient varies with time and space [10]. The effects of chloride binding and multi-directional chloride ingress on chloride diffusion coefficient are also reported [9, 11, 12].

Chlorides diffusing inside the concrete can either be dissolved in the pore solution or chemically and physically bound to the cement hydrates along the diffusion path [9]. Therefore we can divide total chloride into bound and free chloride. It is the free chloride that diffuses to the rebar level and breaks the passive layer that leads to the initiation of reinforcement corrosion [11].The effect of chloride binding in concrete on the corrosion initiation is two-fold: (1) the rate of ionic diffusion of chloride in concrete is reduced, since the amount of available mobile ions (free chloride) is reduced due to binding mechanisms; and (2) the reduction of free chlorides in concrete results in lower amounts of chlorides being accumulated at the reinforcing steel layer [12]. Theoretically, the

concrete matrix gets densified with the passage of time; therefore the chloride binding ability of concrete should also improve based on the same principle. Therefore the effect of chloride binding with age should also be considered in chloride diffusion models.

For considering the effects of chloride binding, multi-dimensional chloride ingress into concrete and densification of concrete due to progress of hydration with time, a suitable partial differential equation (PDE) needs to be proposed which can be solved using numerical analysis for obtaining a more accurate equation of chloride diffusion.

1.2 Need for Research

Chloride diffusion coefficient is one of the key parameters in the prediction of service life of reinforced concrete structures subjected to chloride exposure. The Fick's 2nd law of diffusion is being used to derive the models for chloride diffusion in concrete. However, such models do not include the effects of various significant factors such as chloride binding by the cement, multi-directional ingress of chloride ions, and variation of chloride diffusion coefficient with time due to change in the microstructure of concrete during early period of cement hydration. Therefore, it is required to develop a model that would consider the effects of chloride binding and change in the microstructure with time. The chloride diffusion model developed considering the effect of these factors, relevant to concrete, would enable in predicting the service life of reinforced concrete structures more accurately.

1.3 Objectives

The primary objective of this research is to develop a chloride diffusion model through numerical analysis of basic diffusion equations incorporating the effect of

chloride binding by cement and change in the concrete microstructure with time due to progress of cement hydration. The developed model can be utilized to predict the service life of reinforced concrete structures with more accuracy.

The specific objectives of this study are the following:

1. To plan and conduct an experimental program involving preparation of concrete specimens for exposure to chloride solution and conducting tests to obtain chloride profiles for different exposure periods.
2. To review different diffusion models reported in literature and to develop a model that would incorporate the effects of the chloride binding and densification of microstructure of concrete with time.
3. To develop an approach to solve the proposed model (i.e., differential equation representing the chloride diffusion process) using numerical analysis for calculation of chloride diffusion coefficient and other parameters.
4. To illustrate the application of the developed model in prediction of corrosion initiation time for reinforced concrete structures subjected to chloride exposure.

CHAPTER 2

LITERATURE REVIEW

Voluminous work has been devoted to the various aspects of chloride diffusion, and many researchers studied the durability problems in the Arabian Gulf in the last four decades. The performance of RCC structures in chloride-laden environments is of great importance where a maze of interwoven mechanisms and deterioration synergies are at work. The importance of chloride diffusion in concrete durability is reflected in the tremendous amount of literature devoted to the corrosion of reinforcing steel in concrete. In order to review the work done before related to this study, a detailed literature survey was conducted. For the clarity of presentation, the literature review is divided into the following aspects:

- The influence of chloride binding on chloride diffusion coefficient in OPC and blended (Silica fume) concrete
- The effect of time and space on the chloride diffusion coefficient
- Models currently available for the prediction of service life of RCC structures
- Interaction effect of chloride ingress from more than one side

2.1 The influence of chloride binding on chloride diffusion coefficient

The service life of many structures is affected by chloride induced corrosion. The chloride binding in concrete will affect the rate of chloride ingress which in turn determines the chloride induced corrosion initiation [13]. The pore solution concentration, which is the driving agent of chloride diffusion process, is reduced due to

the chloride binding and the chloride transport process is also slowed down [13]. It is reported that it does not only affect the chloride diffusion but the other mechanisms of chloride ingress (chloride transport from the flow of water due to capillary sorption, wick action, permeation etc.) are also affected due to the binding of chloride [13].

When the binding effect of chloride is considered, the concentration of free chloride is reduced such that the chloride diffusion coefficient is also reduced simultaneously. Therefore the diffusion-reaction model predicts a longer service life than the models that do not consider the effect of chloride binding during the chloride diffusion process [9]. The chloride binding chemical reaction occurs between chloride ions and the C_3A, C_4AF and their hydration products which results in the formation of Friedel's salt as the product of the reaction [10]. It is also reported that chloride binding will be higher with high chloride concentration in the pore solution because chloride ions will have access to the more binding sites [14].

The reduction in chloride diffusion coefficient of blended cement concrete over OPC concrete has been reported [15]. It is reported that 10 to 20 % replacements of micro silica in cements showed a reduction of 2 to 11 times in chloride diffusion coefficient than that of OPC concretes and this significant reduction in silica fume concretes may be attributed to the densification of microstructure due to the development of secondary calcium silicate hydrate in result of pozzolanic reaction [3].

It is significant to consider the chloride binding in the study of the service life of concrete structures. Following are some reasons emphasizing over its importance:

1. It has been reported that only free chlorides (water soluble chlorides) are responsible for corrosion of reinforcement [16,17]

2. Reduction of free chloride concentration in the vicinity of the reinforcement due to chloride binding will reduce the chances of corrosion and thus retarding the diffusion of chloride to the steel level [3,18]
3. The chemical binding of chloride ions with C_3A and C_4AF results in the formation of Friedel's salt, which has a less porous structure and slows down the transport of chloride ions [3]

The chemical reaction between C_3A, C_4AF and chloride ions, which leads to the formation of Friedel's salt, is given below:

$$Ca(OH)_2 + 2NaCl \rightarrow CaCl_2 + 2Na + 2OH$$

$$C_3A + CaCl_2 + 10H_2O \rightarrow C_3A.CaCl_2.10\ H_2O$$

The relative importance of C_3A, C_4AF, C_3S and *w/c* ratio etc. were investigated and the results show that C_3A has the most dominant effect in chloride binding [19]. Various researchers [13,19,20] have suggested models for estimating the chloride binding isotherms with C_3A content depending upon different isotherms (Langmuir isotherm and Freundlich isotherm) and concluded that C_3A content which has an influence on the chloride binding capacity, changes the diffusion coefficient [10]. It was concluded that no single binding isotherm can accurately express the relationship between free and bound chloride within the complete concentration range [14].

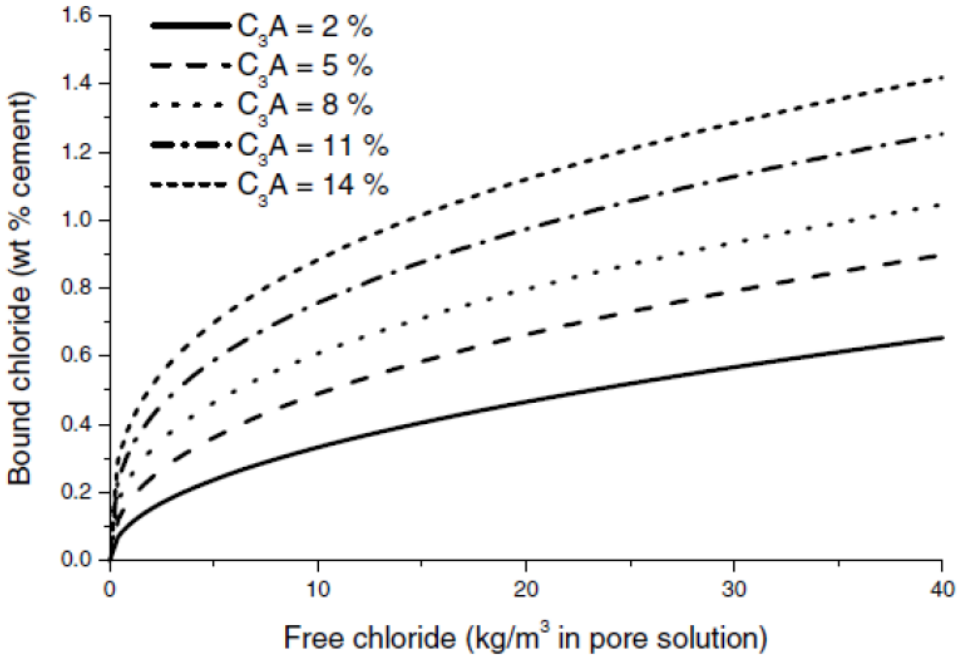

Figure 2.1: Effect of C_3A on chloride binding

2.2 The effect of time and space on chloride diffusion coefficient

The capillary pore structure of concrete changes with *w/c* ratio, degree of hydration, type of cement etc. and it also changes with time at various locations. Therefore both the chloride ion concentration and chloride diffusivity are time and space variables [9]. The chloride diffusion coefficient typically decreases with time because the capillary pore structure is altered due to the continuous formation of hydration products [21]. Figure 2.2 and Figure 2.3 show the schematic images of the relationship between chloride concentration, age and depth with the ongoing chemical and hydration reactions [9].

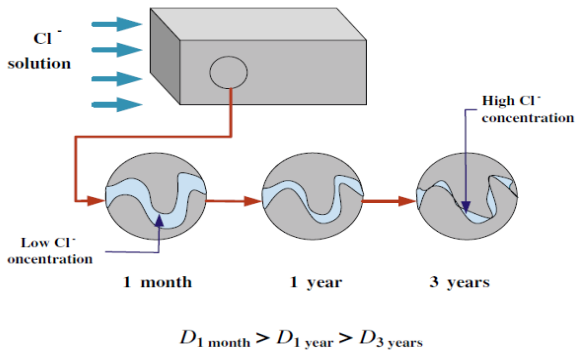

Figure 2.2: Effect of time on chloride diffusion coefficient

Continuing hydration reactions are shown in Figure 2.2, there is an increase in chloride concentration and decrease in diffusion coefficient at a certain depth with increasing time.

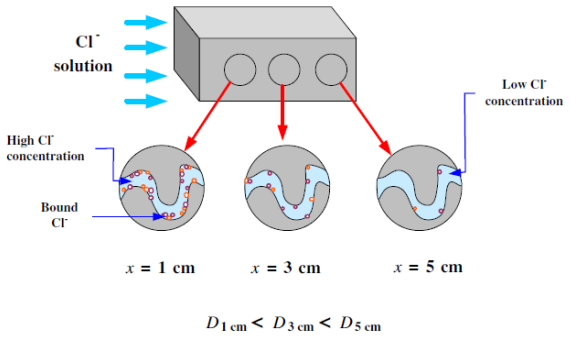

Figure 2.3: Effect of depth (space) on chloride diffusion coefficient

Continuing hydration reactions are shown in Figure 2.3, there is a decrease in chloride concentration and increase in diffusion coefficient with increasing depth at a certain time.

The error function solution given by Crank, for the Fick's 2nd Law of Diffusion (Eq. 2.2) is valid when both the diffusion coefficient (D_c) and the surface concentration (C_s) are assumed constant in time and space. However it is known that D_c varies with space and time due to the variation in concentration itself, temperature, moisture and exposure

conditions [3]. The chloride diffusion coefficient determined by Eq. 2.2 is for certain instances of age and chloride exposure period. For example diffusion coefficient determined after 28 days curing and 50 days exposure to chloride solution will reflect the average concrete properties regarding transportation by diffusion (i.e. from 28^{th} day to 78^{th} day), but this cannot be taken as representative because as the concrete matures, hydration decreases the ion penetration ability, therefore the diffusion coefficient is changing during the exposure period [21]. The diffusivity of concretes with supplementary cementing materials (fly ash, silica fume etc.) is considerably more sensitive to the aging than OPC concrete, and diffusivity of fly ash concrete may be one order of magnitude lower than OPC after approximately 2 years and it is predicted that it may decrease to two orders of magnitude lesser after 100 years! [22].

Ming-Te Liang et al. [23] performed both; total and free chloride analysis for finding the relationship between total and free chloride diffusion parameters, they also reported the variability of both; chloride diffusion coefficient and surface chloride concentration, with time. It was reported that the total and free chloride diffusivities are inversely proportional to the penetration time. Figure 2.4 and Figure 2.5 show the effect of time on chloride diffusion coefficient. It can be observed from Figure 2.4 and Figure 2.5, that both; total and free chloride diffusion coefficients decrease with time. This reduction in diffusion coefficient is very high initially but it steadies after a longer exposure periods. It is therefore, imperative to consider the effect of time, as if the initial (higher) values of diffusion coefficient are used in the analysis; then the results will be very conservative.

.

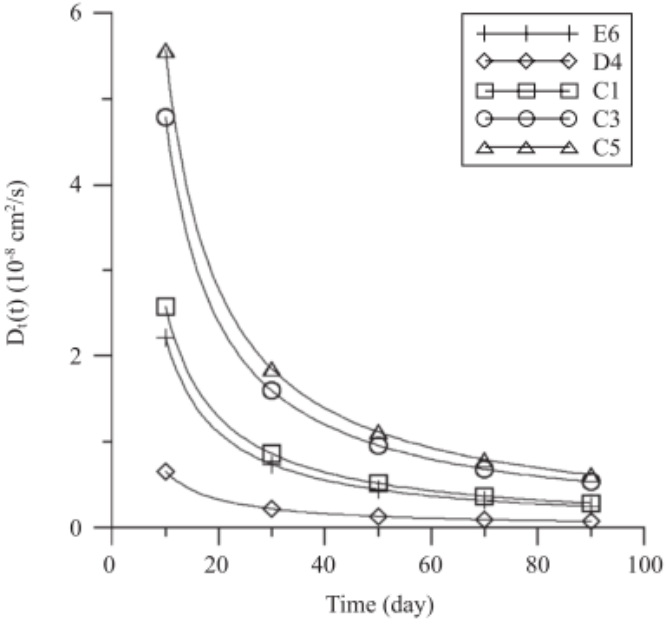

Figure 2.4: Effect of Time on Free Chloride Diffusion Coefficient

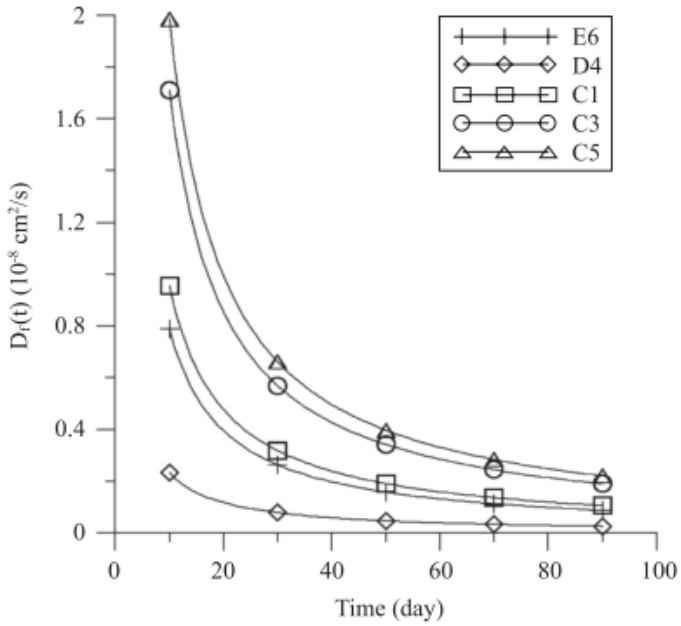

Figure 2.5: Effect of Time on Total Chloride Diffusion Coefficient

Ming-Te Liang et al. [23] also reported the change of diffusion coefficients with increasing penetration depth. It was reported that the total and free chloride diffusivities

are proportional to the square of chloride penetration depth. Figure 2.6 and Figure 2.7 show the change in diffusion coefficients with increasing penetration depth.

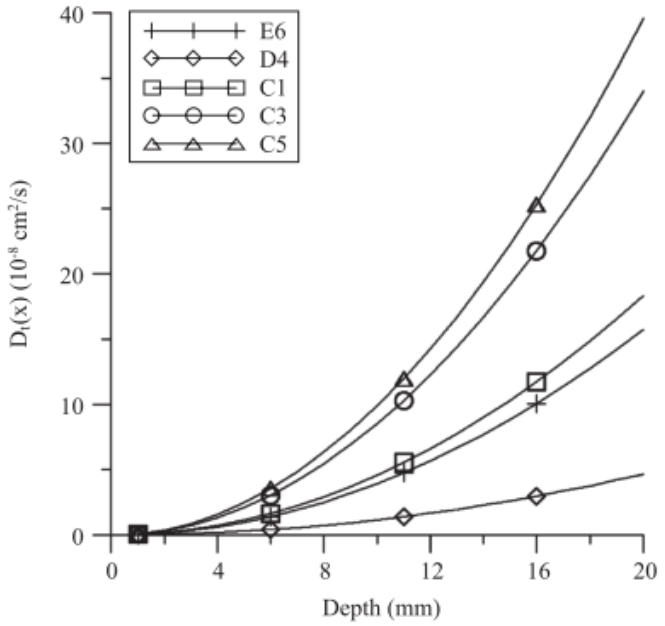

Figure 2.6: Effect of Penetration Depth on Free Chloride Diffusion Coefficient

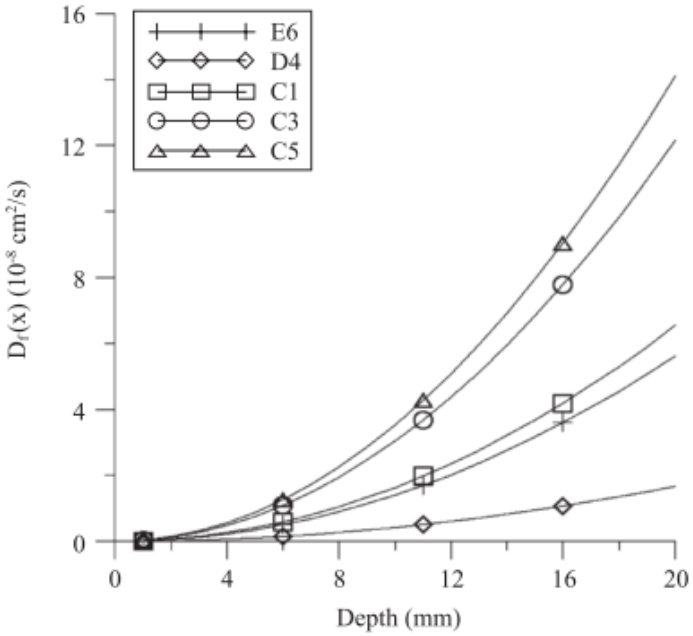

Figure 2.7: Effect of Penetration Depth on Total Chloride Diffusion Coefficient

Therefore, if the chloride diffusion coefficient is considered constant throughout the exposure duration, then the analysis will result in significant error, and the usefulness of simple numerical solution to Fick's 2nd law (Eq. 2.2) for predicting service life of existing structures or for the purpose of designing new structures is questioned [22].

2.3 Models currently available for determination of chloride diffusion coefficient

Due to the prime importance of chloride diffusion coefficient in the durability and service life prediction of RCC structures, considerable efforts have been made by many researchers and different models have been proposed. A simple model which describes the chloride concentration as a function of time and distance under non-steady state is given by Adolf Fick and it is popular by the name of Fick's 2nd law of Diffusion

$$\frac{\partial C}{\partial t} = D\ \frac{\partial}{\partial X}\left(\frac{\partial C}{\partial X}\right) \tag{2.1}$$

With initial condition (*I.C.)* and boundary conditions (*B.C.*) given in Eqs. 2.1.1 through 2.1.3:

I.C.: $C\ (x, 0) = 0$ (2.1.1)

B.C.: $C\ (0, t_m) = C_s$ (2.1.2)

$C\ (x \rightarrow \infty, t_m) = 0$ (2.1.3)

The simple mathematical solution given by Crank that assumes D_a as a constant is

$$C_{x,t} = C_s\left(1 - erf\left(\frac{x}{2\sqrt{D_a t}}\right)\right) \tag{2.2}$$

where,

$C_{x,t}$ = Chloride concentration at depth x and time t,

C_s = Chloride concentration at the surface,

x = depth,

t = time,

D_a = apparent diffusion coefficient.

The values of C_s and D_a are found by least squares [22].

The values so obtained are the average diffusivities of concrete during the period from the start of the exposure to the time of sampling and this approach does not considers the time-dependent changes in chloride diffusion coefficient [22].

B. Martin-Perez et al. [8] proposed a modified Fick's 2nd law which considers the effect of chloride binding by making changes in the computation of chloride diffusion coefficient [8]

$$\frac{\partial C_f}{\partial t} = \frac{\partial}{\partial x}\left(D_c^* \frac{\partial C_f}{\partial x}\right) \tag{2.3}$$

with

$$D_c^* = \frac{D_c}{1 + \frac{1}{\omega_c}\frac{\partial C_b}{\partial C_t}} \quad [m^2/s]$$

where,

D_c^* = apparent diffusion coefficient

Another comprehensive model was developed at University of Toronto which takes into account the multi-mechanic transport process and considers the effect of temperature

and time dependence of the relevant transport coefficient [24,25]. The effect of time is taken as

$$D_t = D_{28} \cdot \left(\frac{t_{28}}{t}\right)^m \tag{2.4}$$

where,

D_t = diffusion coefficient at time t,

D_{28} = diffusion coefficient at time t_{28} (28 days),

m = constant.

Eq. 2.4 accounts for the influence of time on diffusivity and it depends upon the concrete mix variables. Values of m for different concretes have yet to be well established, but some values have been published. The values of m tend to be lower for ordinary Portland cement mixtures than those incorporating mineral additives [21].

Y.-M. Sun et al. [9] developed a model that considers the time/depth and chemical reaction effect on chloride diffusion coefficient. They considered 3 different models:

1. Simple model
2. Time/depth dependent diffusion model
3. Time/depth dependent diffusion-reaction model

The simple model is the one given in the start of this section (Eq. 2.2; solution given by Crank for the Fick's 2nd law of diffusion). In the second model they considered D to be the function of space and time and the proposed model with initial and boundary conditions given in Eqs. 2.5.1 through 2.5.3:

$$\frac{\partial C\ (x,t)}{\partial t} = \frac{\partial}{\partial x}\left(D_{xt}\left(C(x,t)\right)\frac{\partial C(x,t)}{\partial x}\right) \tag{2.5}$$

I.C.: $C\,(x, 0) = C_i$ (2.5.1)

B.C.: $C\,(0, t_m) = C_s$ (2.5.2)

$C(x \rightarrow \infty, t_m) = C_i$ (2.5.3)

Where,

$C\,(x, t)$ and $D_{xt}\,(x, t)$ are the chloride concentration and chloride diffusion coefficient respectively depending on space and time.

The 3rd model presented by Y.-M. Sun et al. [9] also considers the effect of chemical reaction along with the effect of space and time. According to Y.-M. Sun et al. [9] the diffusing chloride ions are assumed to be immobilized by an irreversible first-order chemical reaction and it is given as

$$\ln[C_{xt}^F] = -kt + \ln[C_{xt}^T] \quad (2.6)$$

Where,

k is a constant, and the rate of removal of diffusing chloride ions is k times the free chloride concentration.

Following is the 1-D model given by Y.-M. Sun et al. [9] along with the initial and boundary conditions given in Eqs. 2.7.1 through 2.7.3:

$$\frac{\partial C^F(x,t)}{\partial t} = \frac{\partial}{\partial x}\left(D_{xt,k}^F(C^F(x,t))\frac{\partial C^F(x,t)}{\partial x}\right) - kC^F(x,t) \quad (2.7)$$

I.C.: $C^F\,(x, 0) = C_i^F$ (2.7.1)

B.C.: $C^F\,(0, t_m) = C_S^F$ (2.7.2)

$C^F\,(x \rightarrow \infty, t_m) = C_i^F$ (2.7.3)

Where,

$D^{F}_{xt,k}$ is the free apparent diffusion coefficient of diffusion-reaction equation.

Results for service life prediction are shown in Figure 2.8.

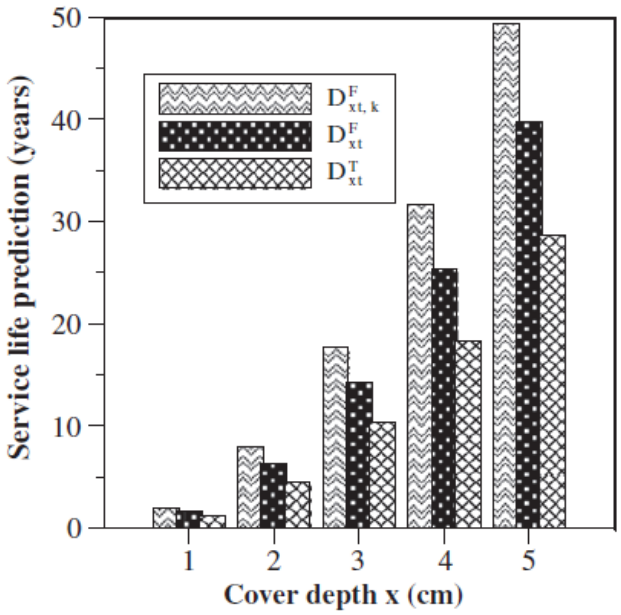

Figure 2.8: Comparison of service life prediction by different Diffusion coefficients

The time/depth diffusion reaction model predicted the highest service life as it considers the chloride binding occurring due to the chemical reaction, and expectedly the simple model predicted the lowest values of service life as it considers the chloride diffusion coefficient as constant and does not account for chloride binding.

Tumidajski [26] considered first order chemical reaction for modeling simultaneous chloride diffusion and chloride binding by introducing reaction term in Fick's 2nd law of diffusion. The model proposed by Tumidajski is given in Eq. 2.8.

$$\frac{\partial C_t}{\partial t} = \frac{\partial}{\partial x}\left(D_t^* \frac{\partial C_t}{\partial x}\right) - kC_t \tag{2.8}$$

I.C.: C (x, 0) = 0 (2.8.1)

B.C.: C (0, t_m) = C_s (2.8.2)

$C(x \rightarrow \infty, t_m) = 0$ (2.8.3)

Tumidajski [26] applied Danckwerts' solution [27] to this model, given in Eq. 2.9

$$C_{t\ (x,t)} = \frac{1}{2} C[\exp\left(-x\sqrt{\frac{k}{D}}\right) erfc\left(\frac{x}{\sqrt{4Dt}} - \sqrt{kt}\right) + \exp\left(x\sqrt{\frac{k}{D}}\right) erfc\left(\frac{x}{\sqrt{4Dt}} + \sqrt{kt}\right)] \quad (2.9)$$

Danckwerts [27] reported that Eq. 2.9 predicts the experimental data well and the fitting of model against experimental data was improved for longer exposure durations.

Walid A. Al-Kutti [3] considered a two-dimensional diffusion model and coupled it with mechanical damage and chloride binding. It was reported that for undamaged concrete D_{eff} was 2.1×10^{-6} mm^2/sec while there was an increase of diffusivity of upto 9 times for the damaged concrete [3].

Bentz et al. [28] performed experiments to investigate the effect of mix variables on chloride diffusion coefficient and concluded that *w/c* ratio, degree of hydration and aggregate volume fraction were the major variables influencing concrete diffusivity.

Zeng [29] developed a 2-D structure to model the chloride diffusion in concrete and treated cement paste and aggregate with different diffusivities. He found that the chloride diffusivity in hetro-structured concrete lag behind that for the homogeneous ones.

2.4 Interaction effect of chloride ingress from more than one side

Through the years of study many valuable results on chloride diffusion in concrete have been obtained and successfully applied in the service life prediction of field concrete structures [30]. However, it was found that most of these results were obtained by studying 1-D chloride diffusion in concrete. But some important locations of concrete structures in the field (edges and corners of beams and columns) are subjected to the

simultaneous attack of 2-D or 3-D chloride ingress [31]. In practical situation, the diffusion rate and degree of deterioration of the edge or corner concrete is larger than that of locations exposed to 1-D [32]. Therefore it is important to study the interaction effect of chloride ingress from more than one side.

Unfortunately, very few literatures are available on 2-D or 3-D chloride diffusion of concrete. Zhang et al. [31] studied the effect of multi-dimensional ingress on chloride diffusion of fly ash concrete and found that the chloride concentration at the same distance of concrete was in order *3-D > 2-D > 1-D*. This suggests that more attention should be paid on the chloride ingress of the edge and corner concrete [31].

CHAPTER 3

RESEARCH METHODOLOGY

The objective of this research is to develop a chloride diffusion model incorporating the effect of chloride binding by cement and change in the concrete microstructure with time due to progress of cement hydration. The developed model can be utilized to predict the service life of reinforced concrete structures with more accuracy.

An experimental program was planned to generate data from the following tests:

1. Total chloride (Acid soluble) concentration
2. Free chloride (Water soluble) concentration

Following tasks were completed to accomplish the objectives of this research:

3.1 Materials

3.1.1 Cementitious Materials

ASTM C 150 Type I Portland cement was utilized in both mixes. For blended cement concrete, 7% silica fume was used as replacement of Portland cement. The chemical composition of the Portland cement and Silica fume is show in the Table 3.1:

Table 3.1: Chemical composition of cementitious materials

Constituent	Weight (%)	
	OPC	**SF**
CaO	64.35	0.48
SiO_2	22	92.5
Al_2O_3	5.64	0.72
Fe_2O_3	3.8	0.96
K_2O	0.36	0.84
MgO	2.11	1.78
Na_2O	0.19	0.5
Equivalent alkalis ($Na_2O + 0.658K_2O$)	0.42	-
Loss on ignition	0.7	1.55
C_3S	55	-
C_2S	19	-
C_3A	10	-
C_4AF	7	-

3.1.2 Aggregates

The coarse aggregates used in this study were crushed limestone from Riyadh Road region. The fine aggregates were dune sand. The specific gravity and absorption of the aggregates are given in Table 3.2:

Table 3.2: Properties of Aggregates

Aggregate	Absorption (%)	Bulk Specific Gravity
Coarse Aggregate (Riyadh Road)	2.05	2.45
Fine Aggregate (Dune Sand)	0.6	2.66

ASTM C 33 No. 7 Grading was used for coarse aggregates. The particle size distribution of coarse aggregates is given in Table 3.3:

Table 3.3: Particle size distribution of Coarse Aggregates

SIZE (mm)	% Retained	Cumulative (% Retained)	Cumulative (% Passing)	ASTM C 33 (No.7 Grading)
19	0	0	100	100
12.5	10	10	90	90-100
9.5	40	50	50	40-70
4.75	40	90	10	0-15
2.36	10	100	0	0-5

3.2 Concrete Mix Variables

The concrete mixes were prepared with the following variables:

a) Cementitious material content: 400 kg/m^3 (same in all the mixes)

b) Water to cementitious material ratio (*w/cm*): 0.4 for OPC concrete and Silica fume cement concrete

c) Coarse to fine aggregate ratio: 1.5 (same in all the mixes)

The details are summarized in the Table 3.4:

Table 3.4: Details of concrete mix variables

Sr. No	Variable	Levels	Total no. of Levels
1	*w/c* Ratio	*w/c* of 0.4 OPC and 7% Silica fume Blended concrete	1
2	Cementitious Material content	400 kg/m^3	1
3	Exposure type	3 types (Exposure from 1 face, 2 adjacent faces and 3 adjacent faces)	3
4	Exposure duration	50, 120 and 165 days	3

3.3 Mix design

ACI Absolute Volume Method was used for Mix design. The weights of ingredients for both concrete mixes are given in Table 3.5:

Note: (An adequate amount of Superplasticizer, Glenium 51 was added to achieve the slump of about 75 mm)

Table 3.5: Summary of weights of ingredients for various concrete mixes

Mix No.	w/c	Cement (kg/m^3)	Silica fume (kg/m^3)	Water Content (kg/m^3)	Coarse aggregate (kg/m^3)	Fine aggregate (kg/m^3)
1	0.4	400.0	0.0	186	1044	696
2	0.4	372.0	28.0	185	1038	692

3.4 Preparation of Concrete Specimens

The following concrete specimens were cast from each concrete mix:

i. Cube specimens (100 mm) for the determination of compressive strength

ii. Cube specimens (150 mm) for chloride diffusion exposure

The concrete constituents were mixed in a revolving drum mixer for approximately three to five minutes to obtain uniform consistency. Glenium 51 Superplasticizer was added to enhance the workability and to keep the slump around 75 mm. After mixing, the concrete was filled in the moulds in 3 layers and was vibrated over a vibrating table to achieve adequate compaction.

Figure 3.1: Slump of Mix No. 1

3.5 Curing and chloride exposure

After casting, the samples were moist cured in laboratory conditions for 28 days at 22 $\pm$ 3 °C. Thereafter, they were allowed to dry in the laboratory conditions (22 $\pm$ 3 °C) for seven days to drive out the moisture and then coated with an epoxy resin on the sides of cubes to allow one dimensional and two dimensional diffusion of chloride ions through the uncoated surfaces. The coated specimens were then immersed in *5%* sodium chloride solution and they were tested at three different time steps (50, 120 and 165 days).

Figure 3.2: Epoxy coating on specimens

Figure 3.3: Epoxy coated specimens for different exposures

Figure 3.4: Epoxy coated specimens exposed to 5% NaCl solution

3.6 Laboratory Testing

The concrete specimens were tested to evaluate the following properties:

- Compressive strength
- Free chloride concentration
- Total chloride concentration

3.6.1 Compressive Strength

Compressive strength was determined using 100 mm cube specimens according to ASTM C 39 [33].

Figure 3.5: Compressive strength testing

3.6.2 Free Chloride Concentration

150 mm cube specimens were exposed to 5 % NaCl solution for 3 time steps (T1 = 50, T2 = 120 and T3 = 165 days). The specimens were exposed to 3 different exposure conditions; 1D exposure (5 faces were epoxy coated and one face was left open), 2D2 exposure (2 adjacent faces were left open and the remaining 4 faces were epoxy coated) and 2D3 exposure (3 adjacent faces were left open and the remaining 3 faces were epoxy coated). Table 3.6 shows the details of concrete mixtures, exposure conditions and exposure duration.

Table 3.6: Details of Chloride profile designations

Designation	Concrete Mix No.	Exposure condition	Exposure duration (days)
M1-1D-T1	1	1-dimensional	50
M1-2D2-T2	1	2-dimensional, 2 adjacent sides	120
M2-2D3-T3	2	2-dimensional, 3 adjacent sides	165

Figure 3.6 through Figure 3.8 show the different exposure conditions. At the end of each exposure tenure, specimens were taken out of the chloride solution and 50 mm diameter cores were extracted from each exposed face. For every concrete mix, 6 cores (1 core for 1D, 2 cores for 2D2 and 3 cores for 2D3) were extracted at each time step. Slices of 5mm thickness were obtained at 6 different depths (0-5, 8-13, 16-21, 24-29, 40-45 and 48-75 mm) by cutting the cores using concrete cutting machine. The depths at which the cores were sliced to obtain chloride profile are given in Table 3.7. Theses slices were pulverised to obtain powder samples passing through ASTM No. 100 seive. The powdered samples were then analyzed for both *free* chloride (water soluble chloride) and *total* chloride (acid soluble chloride).

Table 3.7: Depth of Slices for Chloride Profile

Slice No.	Depth (mm)	Average depth for analysis (mm)
1	0-5	2.5
2	8-13	10.5
3	16-21	18.5
4	24-29	26.5
5	40-45	42.5
6	48-75	61.5

Figure 3.6: Specimen Subjected to Chloride Exposure from Two Adjacent Sides

Figure 3.7: 50 mm Cores Extracted from the Two Exposed Faces

Figure 3.8: 50mm Core Extracted from Specimen Exposed to 1D Chloride Ingress

The procedure for finding the water soluble (free) chloride concentration is given below:

1. 3 gms of powdered sample was taken into the beaker
2. 50 ml of hot distilled water (100^{o} C) was added and the mixture was thoroughly stirred and left for 24 hours for the digestion of chloride
3. The solution was filtered into the flask and the filtrate was made 100 ml by adding distilled water
4. 0.2 ml of the solution was taken through micro pipette and 9.8 ml of distilled water was added into it for making it 10ml
5. After that, 2 ml each of 0.25 M ferric ammonium sulphate and mercuric thiocyanate was added into that 10 ml solution
6. Solution was gently shaken and was taken into the a test tube

7. The test tube was placed into the spectro-photometer (set at 460 nm wave length) and the absorbance value was measured
8. Finally, the free chloride concentration was calculated using chloride calibration curve

3.6.3 Total Chloride Concentration

The steps for calculating total chloride concentration are exactly the same except the digestion procedure of total chlorides. Following are the steps involved in the digestion of total chlorides

1. 3 gms of powdered sample was taken into the beaker
2. 25 ml of hot distilled water was added into it and stirred thoroughly
3. 3 ml of concentrated Nitric acid was added
4. The solution was then heated over a hot plate and taken away just before boiling

This completes the digestion of total chlorides and the rest of the procedure was same as that of free chloride concentration.

Figure 3.9: Extracting 2” core from exposed faces of specimens

Figure 3.10: Cutting slices at different depths of extracted cores for chloride analysis

Figure 3.11: Samples left for filtration after digestion of chlorides

3.7 Development of diffusion model

The Fick's 2nd law of diffusion has been used for long time to derive the models for chloride diffusion in concrete. However, most of the models derived and reported in the literature do not include the effects of various significant factors such as chloride binding by the cement, multi-directional ingress of chloride, and variation of chloride diffusion coefficient with time due to change in the microstructure of concrete. As mentioned earlier, recently some research works have been reported which have addressed these factors in the chloride diffusion modeling. However, the effects of two major factors (i.e., chloride binding and time) on chloride diffusion coefficient have not been considered simultaneously.

In order to model the actual behavior of chloride diffusion in concrete with more accuracy, it is necessary to incorporate these both factors together in the diffusion model. The time effect is incorporated in the proposed model by introducing a time reduction factor with chloride diffusion coefficient. Therefore the chloride diffusion coefficient is no more a constant but it reduces with the passage of time. The effect of binding of chloride ions with cement and its products is incorporated in the proposed model by introducing a constant term "*k*"; which represents the binding of chloride ions. The proposed model is presented in Eq. 3.1

$$\frac{\partial C}{\partial t} = Df(n)\frac{\partial^2 C}{\partial x^2} - kC \tag{3.1}$$

With initial and boundary conditions given in Eqs. 3.1.1 through 3.1.3:

I.C.: $C\,(x, 0) = 0$ (3.1.1)

B.C.: $C\,(0, t) = C_s$ (3.1.2)

$$\frac{\partial C}{\partial x}\,(x \rightarrow \infty, t) = 0 \tag{3.1.3}$$

Where,

D = Chloride Diffusion coefficient (cm^2/s)

$f(n)$ = Time reduction function (detail explanation in Chapter 4, Sec. 4.2.3)

k = Chloride binding factor (s^{-1})

Equation 3.1 was numerically solved as a *boundary value problem in space* and as an *initial value problem in time* with the above initial and boundary conditions.

In real life, reinforced concrete structures are exposed to multi-directional chloride diffusion. The synergic effect of simultaneous exposure from more than one side can lead

to a faster rate of deterioration and the critical members may show signs of distress much earlier than predicted. Hence, it is necessary to consider this effect in order to mimic the true behavior of chloride diffusion. Unfortunately, these effects cannot be considered by one-dimensional chloride diffusion analysis. Figure 3.12 show the schematic of the interaction of chloride diffusion at the corners of a structural members and the path of maximum interaction is represented by red dots:

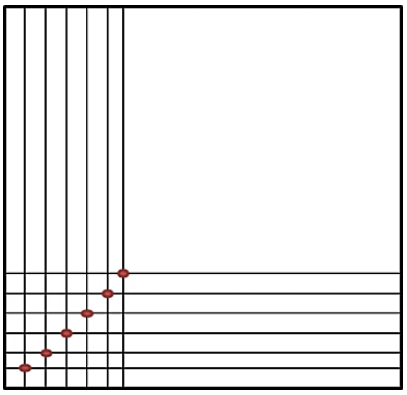

Figure 3.12: Interaction effect of chloride diffusion from 2-sides

The chloride front is diffusing inside the concrete from both faces, at the edges the concentration from both sides is interfered and increased. Due to the synergic effect the threshold chloride concentration will be attained at the corner reinforcements much earlier than the side reinforcements (although the cover depth is more at the corner reinforcement). This phenomenon of interaction cannot be evaluated while considering the uni-directional chloride ingress. Therefore experimental data is obtained by simulating different boundary conditions thorough simultaneously exposing more than one faces of concrete cubes to chloride solution, hence simulating 2-dimensional chloride attacks.

CHAPTER 4

MODELING OF CHLORIDE DIFFUSION

In this chapter the chloride diffusion models are explained in detail. All the models were solved using Wolfram Mathematica 9.0 [34]. The data of free and total chloride concentrations were obtained for 3 exposure periods and 6 different depths for each type of exposure condition for all mixes. The data was inputted in the software and then the models were solved numerically to obtain diffusion parameters. Table 4.1 shows the different depths and exposure periods at which the chloride concentrations were obtained:

Table 4.1: Exposure periods and depths of chloride concentration

Exposure periods (days)	Sampling depths (cm) after each exposure period
50, 120 and 165	0.25
	1.05
	1.85
	2.65
	4.25
	6.15

4.1 Inputting Data in the Software

Chloride concentration data was inserted into the software in an orderly manner i.e. {depth (cm), exposure period (day), chloride concentration (% by wt. of cement)}. A typical example of inputting data for one of the exposure sample is given below:

Tdata = {{0.25, 50, 1.337}, {1.05, 50, 0.698}, {1.85, 50, 0.577}, {2.65, 50, 0.402}, {4.25, 50, 0.270}, {6.15, 50, 0.225}, {0.25, 120, 1.613}, {1.05, 120, 0.852}, {1.85, 120, .354}, {2.65, 120, 0.267}, {4.25, 120, 0.061}, {6.15, 120, 0.061}, {0.25, 165, 1.726}, {1.05, 165, 0.668}, {1.85, 165, 0.413}, {2.65, 165, 0.282}, {4.25, 165, 0.182}, {6.15, 165, 0.011}};

The first 6 bracketed terms represent the data for 1st exposure period (50 days) similarly the second 6 terms represent the 2nd exposure period (120 days) and finally the last 6 terms represent the 3rd exposure (165 days). Moreover, the values of depth were inputted in an ascending order along with their chloride concentration values.

4.2 Chloride Diffusion Models

For the clarity of presentation each model is explained in a separate sub-section.

4.2.1 Fick's Second Law of Diffusion - 1st Model

As discussed in Section 2.3 Crank gave solution of Fick's 2nd Law of Diffusion (Eq. 2.2) which considers diffusion coefficient (D) as a constant:

$$C_{x,t} = C_s\left(1 - erf\left(\frac{x}{2\sqrt{Dt}}\right)\right) \quad \text{(Eq. 2.2)}$$

Eq. 2.2 comprises of two unknowns; Diffusion coefficient (D) and surface concentration (C_s). Therefore the Eq. 2.2 was used to fit the data for the two unknowns D and C_s by using "***FindFit***" command in Mathematica. Once the values of D and C_s are obtained then the same equation can be solved to predict the time of onset of corrosion (time taken by the chloride ions to attain the threshold concentration at rebar level). Table 4.2 shows the cover depth and threshold chloride concentration values considered in this study:

Table 4.2: Cover depth and Threshold Chloride concentration

Cover Depth (cm)	Threshold Chloride Concentration (% wt. of Cement)	
5	**Free Chloride**	**Total Chloride**
	0.15	0.2

Mathematica has a built-in function "***FindRoot***"; which is used to calculate the time of onset of corrosion by putting the cover depth and threshold chloride concentration in the Model.

FindRoot [M1 = 0.035 /. x → 5, {t, 200.}]

Where,

M1 represents the Model 1, 0.035 is the threshold chloride concentration by % wt. of concrete (equivalent to 0.2 % by weight of cement for 400 kg/m^3 cementitious material). ***x*** = 5 cm is the cover depth and ***t*** = 200 days is an initial guess. From this command the time for threshold chloride concentration at rebar level (*service life*) was obtained.

4.2.2 Fick's 2nd Law of Diffusion considering the effect of time - 2nd Model

Fick's 2nd law of diffusion considers chloride diffusion coefficient (*D*) as a constant however it was reported that *D* decreases with time due to change in micro-structure. This was evident from different values of *D* calculated using Model 1 for different exposure time (Table 5.2 through Table 5.5). It was observed that *D* at 120 days of exposure period (D_{120}) attains half of the value of what it was at 50 days exposure (D_{50}). The decrease in *D* was rapid initially but this change attenuates with the passage of time and *D* tends to achieve a stable value after a long period of time. Table 4.3 show the

values of *D* at 3 different exposure periods for one of the exposure condition in concrete mixture M2:

Table 4.3: Diffusion Coefficients at different time steps

Exposure Period (days)	***D* in 10^{-8} cm^2/sec**
50	22.94
120	9.05
165	6.07

It can be observed from Table 4.3 that the decrease in *D* between 50 to 120 days exposure is more than 100%, but this decrease was attenuated to less than 33% between 120 and 165 days. This behavior was captured by introducing a time dependent function, $f\ [t]$, with *D*. Eq. 4.1 represents this function:

$$f[t] = \left(\frac{a+bt}{t}\right)^n \qquad \text{(Eq. 4.1)}$$

Eq. 4.1 was trained to mimic the observed behavior by using "***NSolve***" built-in function in Mathematica.

eq1 = f [t] = 1 (@ t = 50 days)

eq2 = f [t] = 0.5 (@ t = 120 days)

Sol = NSolve [{eq1, eq2}]

The constants *a* and *b* were obtained from the solution. The value of n varies between 0.2 and 2.0 with an increment of 0.2. The software gives the liberty of plotting the behavior of function (Eq. 4.1) for different values of *n*. A typical plot of Eq. 4.1 for *n* = 1.8 is shown in Figure 4.1:

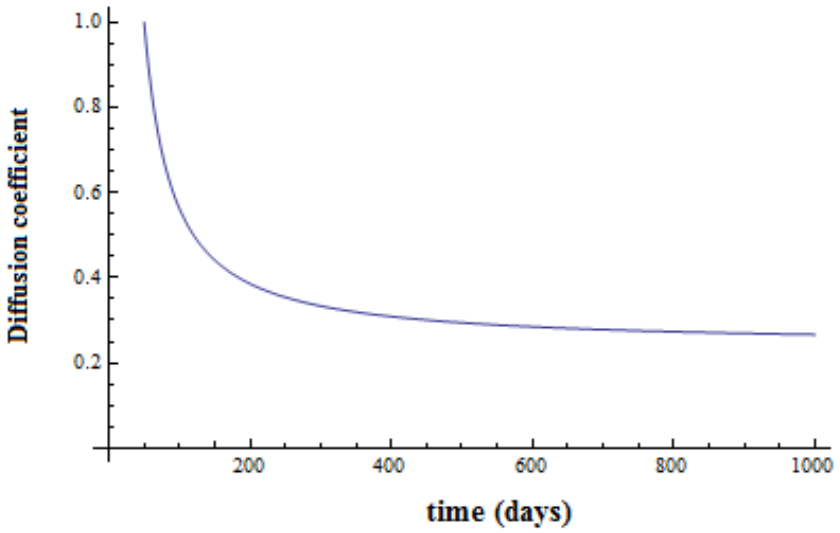

Figure 4.1: Variation of *D* with time

For example, In Figure 4.1, *D* is taken as 1 at 50 days and the value of *D* decreases rapidly for the first 200 days but then the change in curvature is minimized and *D* attains a sought of a stable value.

Therefore, the 2nd Model is again a Fick's 2nd Law of diffusion including the effect of time on *D*. The modified model is presented in Eq. 4.2:

$$\frac{\partial C}{\partial t} = Df(t)\frac{\partial^2 C}{\partial x^2} \tag{4.2}$$

With initial and boundary conditions given in Eqs. 4.2.1 through 4.2.3:

I.C.: $C\,(x, 0) = 0$ (4.2.1)

B.C.: $C\,(0, t) = C_s$ (4.2.2)

$\frac{\partial C}{\partial x}\,(x \rightarrow \infty, t) = 0$ (4.2.3)

Where,

$f(t)$ = Time reduction function considering the effect of continuous hydration

D = Chloride Diffusion coefficient

The differential equation (Eq. 4.2) was fitted numerically by using a built-in function "***NDSolve***" in Mathematica for the available experimental data to evaluate the diffusion parameters D and C_s. Initial guesses are required for the unknown variables when numerical fitting operation is performed. Therefore the values obtained from 1st model were used as the starting point and inputted as the initial guesses in 2nd model.

Once the diffusion parameters were evaluated from the experimental data, then the same model was again used with the obtained values of D and C_s, and the model was trained for the larger exposure periods. This is synonymous to extrapolating the behavior of the model. It is necessary to perform this extrapolation of the model so that we can predict the diffusion behavior and the time of onset of reinforcement corrosion.

It was observed that by incorporating the effect of densification of micro-structure with time on diffusion coefficient, the amount of chloride diffusing at rebar level with time was significantly reduced as can be seen from Figure 4.2.

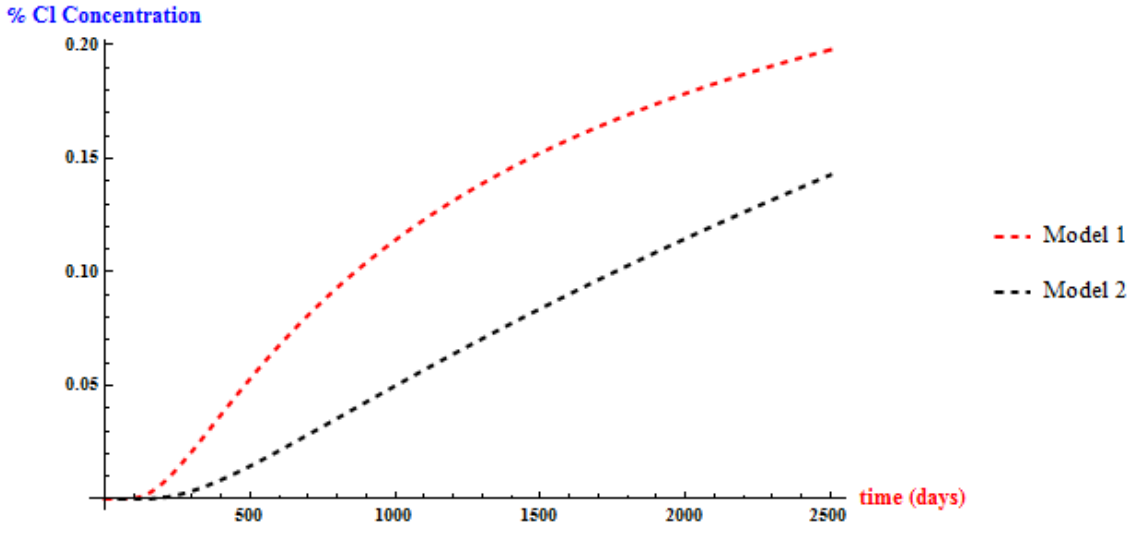

Figure 4.2: Comparison of Models 1 and 2

4.2.3 Fick's 2nd Law of Diffusion considering the effect of time and chloride binding - 3rd Model

In Sec. 4.2.2 the effect of incorporating the time dependent diffusion coefficient was observed. Moreover, it has been reported that the pore solution concentration, which is the driving agent of chloride diffusion, is reduced due to the chloride binding and therefore the chloride transport process is also slowed down [13]. It is also reported that if the binding effect of chloride is considered, the concentration of free chloride ions is reduced affecting the chloride diffusion coefficient. Therefore, the diffusion-reaction model predicts a longer service life than the models that do not consider the effect of chloride binding during the chloride diffusion process [9].

The proposed chloride diffusion model incorporating the effects of time and chloride binding is given by Eq. 4.3, as follows:

$$\frac{\partial C}{\partial t} = Df(t)\frac{\partial^2 C}{\partial x^2} - kC \tag{4.3}$$

With initial and boundary conditions given in Eqs. 4.3.1 through 4.3.3:

I.C.: C (x, 0) = 0 (4.3.1)

B.C.: C (0, t) = C_s (4.3.2)

$\frac{\partial C}{\partial x}$ (x→ ∞, t) = 0 (4.3.3)

Where,

D = Chloride Diffusion coefficient

$f(t)$ = Time reduction function considering the effect of continuous hydration

k = Chloride binding factor

Model 3 does not only incorporates the effect of continuous hydration but it also takes into the account the binding of chloride ions with hydration reactions.

The procedure followed for solving the Model 3 is similar to that of followed for Model 2 and explained in Sec. 4.2.2. The only difference is that, 3rd Model has 3 unknown parameters D, C_s and k. As stated earlier that the built-in function "***NDSolve***" in Mathematica requires initial guesses of unknown parameters for fitting the model. The first two values (D and C_s) will be obtained from Model 1 but "k" is not obtained by it. The problem is tackled by using the experimentally generated data. In this study the experimental data was obtained for both total and free chloride concentrations. Therefore the amount of chloride binding is calculated by subtracting the values of free chloride concentration from total chloride concentration values:

Bound Chloride = Total chloride – Free chloride (4.4)

Once the values of bound chloride concentration are obtained, then these values can be divided by the exposure period to obtain the chloride binding frequency in terms of days. e.g.:

k = (Total chloride – free chloride) / exposure duration (4.5)

From Eq. 4.5 an educated guess for k can be obtained which can then be inserted in Mathematica for fitting the Differential equation (Model 3).

Y.-M. Sun et al [9] reported that diffusion reaction models predicts the higher service life than the models which do not consider the effect of binding reactions. It was verified as Model 3 predicted the highest values of onset of corrosion and the amount of chlorides diffused to the rebar level with time were the lowest, as can be seen from Figure 4.3:

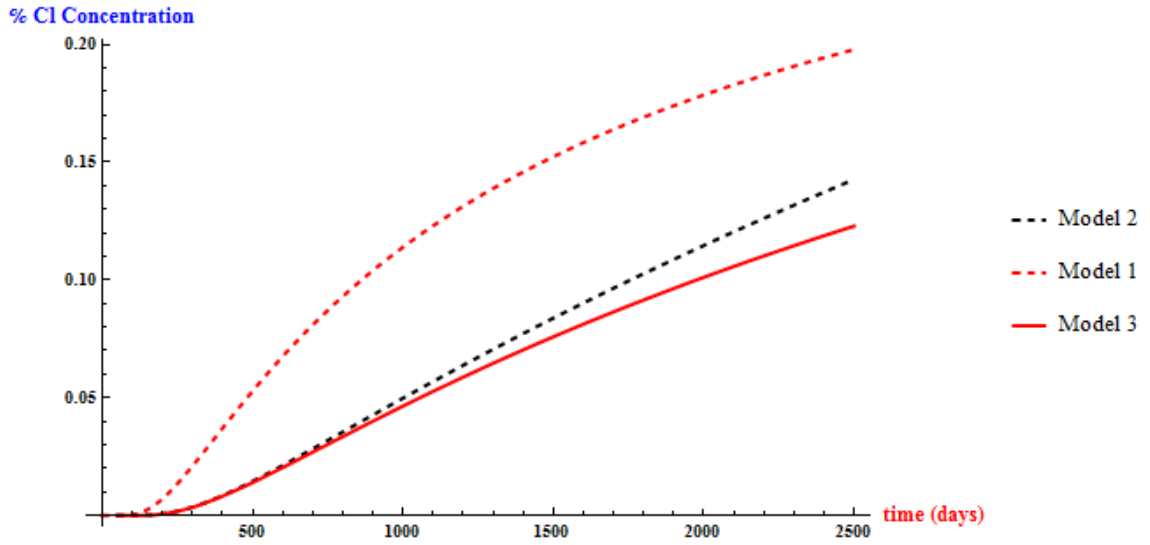

Figure 4.3: Comparison of Models 1, 2 and 3

4.2.4 Analytical solution of Fick's 2nd Law of Diffusion considering the effect of chloride binding - 4th Model

Diffusion Reaction model has been used by Tumidajski [26] for incorporating the effects of chemical reaction and chloride binding. However, this model does not consider the effect of time on diffusion coefficient and considers *D* as a constant. The proposed model by Tumidajski [26] is presented in Eq. 4.6:

$$\frac{\partial C}{\partial t} = D\frac{\partial^2 C}{\partial x^2} - kC \tag{4.6}$$

With initial and boundary conditions given in Eqs. 4.6.1 through 4.6.3:

I.C.: $C\,(x, 0) = 0$ (4.6.1)

B.C.: $C\,(0, t) = C_s$ (4.6.2)

$C\,(x \rightarrow \infty, t) = 0$ (4.6.3)

Where,

D = Chloride Diffusion coefficient

k = Chloride binding constant

The model presented in Eq. 4.6 is similar to Model 3 (Eq. 4.3) except that in Eq. 4.3; D is a function of time whereas in Eq. 4.6, D is taken to be a constant. Tumidajski [26] applied Danckwerts solution [27] to the Eq. 4.6. The solution is given in Eq. 4.7:

$$C_{t\ (x,t)} = \frac{1}{2} C\left[\exp\left(-x\sqrt{\frac{k}{D}}\right) erfc\left(\frac{x}{\sqrt{4Dt}} - \sqrt{kt}\right) + \exp\left(x\sqrt{\frac{k}{D}}\right) erfc\left(\frac{x}{\sqrt{4Dt}} + \sqrt{kt}\right)\right] \qquad \text{(Eq. 4.7)}$$

Eq. 4.7 was fitted in Mathematica by using built-in function "***FindFit***" for evaluating the unknown diffusion parameters D, C_s and k. Similarly, the model's behavior was extrapolated for larger values of time to predict the time for onset of corrosion. The service lives predicted by Model 4 were higher than Model 1. It was expected because Model1 does not incorporate the chloride binding which reduces the free chloride ions concentration and delays the onset of corrosion. However, the predicted service lives by Model 4 were lower than Models 2 and 3 because of neglecting the effect of time on chloride diffusion coefficient. Figure 4.4 shows a typical plot of chloride concentration of Models 1, 2, 3 and 4 at rebar level with time:

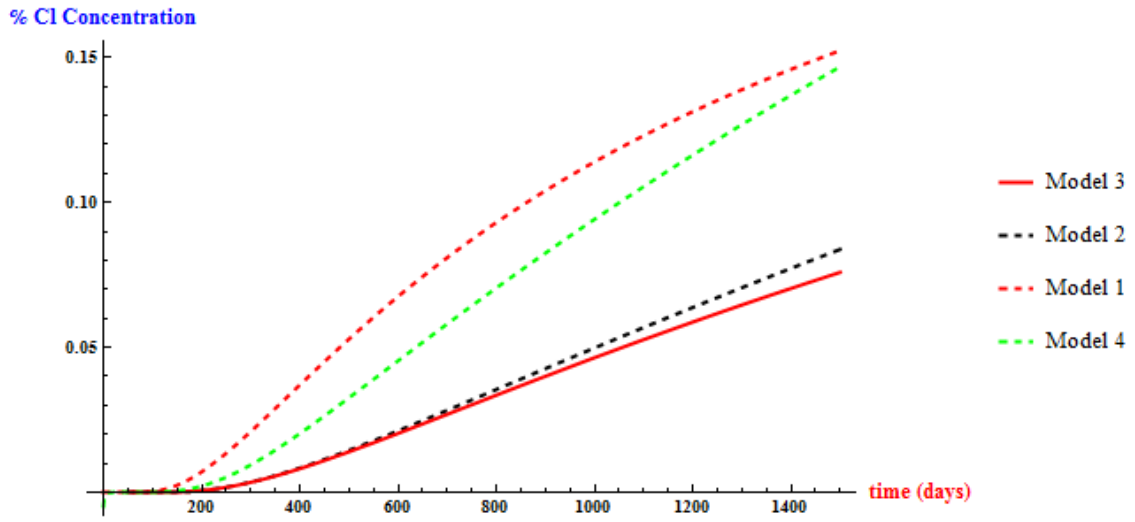

Figure 4.4: Comparison of Models 1, 2, 3 and 4

4.2.5 Analytical solution of Fick's 2nd Law of Diffusion considering the effect of chloride binding with new BC's - 5th Model

The same diffusion reaction model presented in Section 4.2.4 (Model 4) which is proposed by Tumidajski [26] for incorporating the chemical reaction and chloride binding was solved analytically for having an explicit expression of chloride concentration. Despite, this model has an explicit solution given by Danckwerts [27]; the model was revisited to address the wider pool of boundary conditions.

The initial and boundary conditions used in the solution of Model 5 are given in Eqs. 4.8.1 through 4.8.3:

I.C.: $C\,(x, 0) = 0$ (4.8.1)

B.C.: $C\,(0, t) = C_s$ (4.8.2)

$\frac{\partial C}{\partial x}\,(x \rightarrow \infty, t) = 0$ (4.8.3)

It is to be noted that in Model 4, the BC's used by Danckwerts [27] were:

$C\ (0, t) = C_s$ (4.6.2)

$C\ (x \rightarrow \infty, t) = 0$ (4.6.3)

The necessity for modifying these BC's occurs due to the multi-directional chloride ingress. This could be explained with the help of Figure 4.5:

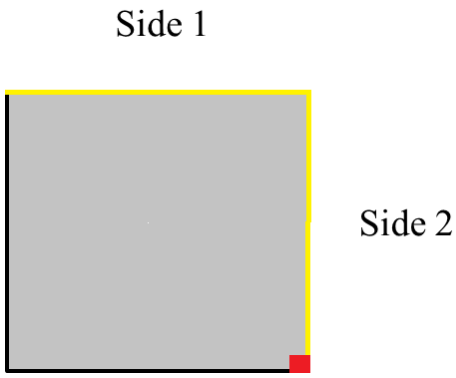

Figure 4.5: Multi-directional Chloride exposure in Concrete Structures

Concrete structures are exposed to multi-directional chloride attack in real life. In Figure 4.5 sides 1 and 2 are exposed to chloride solution (represented by yellow lines). Suppose Danckwerts' BC's are applied at side 1 [$C(x \rightarrow \infty, t) = 0$] then the face opposite to side 1 will be having $C = 0$ along its entire length. This will violate the BC [$C\ (0, t) = C_s$] for side 2 because at the edge (represented by Red dot in Fig. 4.5); the value of concentration cannot be zero and C_s at the same time. Therefore, it is more appropriate to define slope of concentration equals to zero ($\frac{\partial C}{\partial x} = 0$) rather than concentration itself equals to zero ($C = 0$). Based on this explanation, Eq. 4.6 was solved by applying new BC's and the solution is given in Eq. 4.8:

$$\mathrm{Ct}\ (x, t) = \mathrm{Cs}\left(\frac{e^{-\alpha\xi}\left(e^{2\alpha}+e^{2\alpha\xi}\right)}{1+e^{2\alpha}} + \mathrm{Sum}\left[-\frac{4n\pi}{n^2\pi^2+4\alpha^2}\, e^{\left(-\frac{1}{4}n^2\pi^2-\alpha^2\right)\tau}\, \mathrm{Sin}\left[\frac{n\pi\xi}{2}\right]\right]\right) \quad \text{(Eq. 4.8)}$$

Where,

C_t (x, t) = Cl. Concentration at depth "x" and time "t"

C_s = Surface Cl. Concentration

n = No. of terms in Sine series i.e. 21, 31….. etc.

$$\xi = \frac{x}{L}$$

$$\tau = \frac{D\ t}{L^2}$$

$$\alpha = \sqrt{\frac{k\ L^2}{D}}$$

$\boldsymbol{\xi}, \boldsymbol{\tau}$ and $\boldsymbol{\alpha}$ are dimensional-less constants.

Eq. 4.8 was fitted numerically in a similar way as Eq. 4.7 for evaluating diffusion parameters D, C_s and k. Although, the solutions obtained by Models 4 and 5 were different, and were obtained by different sets of BC's; but their behavior was quite similar and the values obtained from both these models were very close to each other. This serves as a check that the proposed solution solved with new BC's is correct and applicable. Figure 4.6 shows a typical plot of chloride concentration of all 5 Models at rebar level with time:

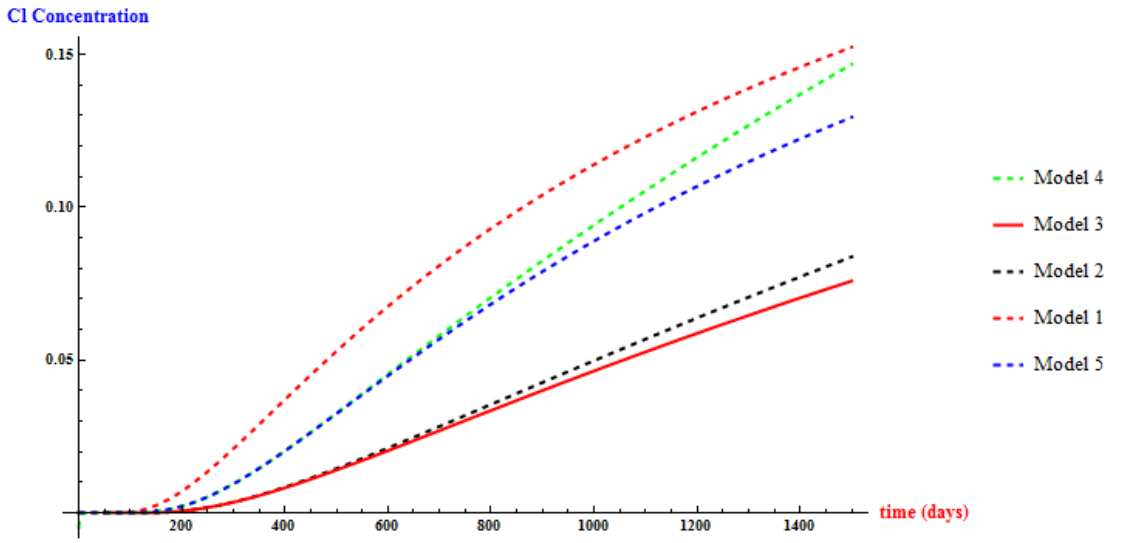

Figure 4.6: Comparison of all 5 Models

Section 4.2 presented the details of all the Models solved and employed in this study. Starting from the very basic Crank's solution to the analytical solution of differential equation incorporating chloride binding effect; the behavior of each model was observed. It was observed that, by using simple Crank's solution (Eq. 4.2), the service life of concrete structures is underestimated because of neglecting the effects of chloride binding and densification of microstructure with time. The service life values were increased by the incorporation of chloride binding effect only (as observed in Models 4 and 5). But there was a significant increase in time of onset of corrosion, when change in diffusion coefficient due to densification of microstructure was incorporated (i.e. Models 2 and 3). Table 4.4 presents the times of onset of corrosion of one of the exposure conditions of concrete mixture 1, computed by all models:

Table 4.4: Comparison of Service lives obtained from different Models

Model No.	Time (Days)	Service life in terms of Model 1
1	387	1
2	793	2.05
3	822	2.12
4	518	1.34
5	520	1.34

From these 5 Models, *Model 3* is proposed to be the most appropriate because it considers the effects of both chloride binding and change in diffusion coefficient due to the densification of microstructure with time.

CHAPTER 5

RESULTS AND DISCUSSION

In this chapter the results of experimental work and Numerical Modeling are discussed. For simplicity and clarity of presentation, the results are presented under individually devoted sections.

5.1 Compressive Strength test Results

Compressive strength test was performed on the 100 mm cube sample after 28 days of curing. The results of compressive strength are shown in Table 5.1. The compressive strength test results indicated that the both concrete mixtures had almost similar high strength grade.

Table 5.1: 28 days Compressive Strength

Mix No.	Cementitious Material	f_c' at 28 days (MPa)
1	100 % OPC	51.62
2	7 % Silica fume + 93 % OPC	52.22

5.2 Free Chloride and Total Chloride Profiles

The chloride profiles for both *free* and *total* chloride concentrations are shown in Figure 5.1 through Figure 5.18 for both concrete mixtures M1 and M2. As expected, in all cases the *total* chloride concentration is more than *free* chloride concentration due to the chloride binding through chemical and physical actions taking place between external chloride ions and C_3A and C-S-H gel inside the concrete. It was also observed that the

chloride concentration values including surface concentration were increasing with the time.

The chloride profiles shown in Figure 5.11 through Figure 5.18 for mixture M2 containing silica fume, indicates the higher chloride binding capacity as compared to the mixture M1 without silica fume. This is because the silica fume concrete has more denser micro-structure, which results in greater amount of chloride ions physically adsorbed to the hydration products. Secondly, it was noted that although the amount of C_3A is less in M2, due to 7% replacement of cement with silica fume but the effect is less promoninet due to the small replacement percentage.

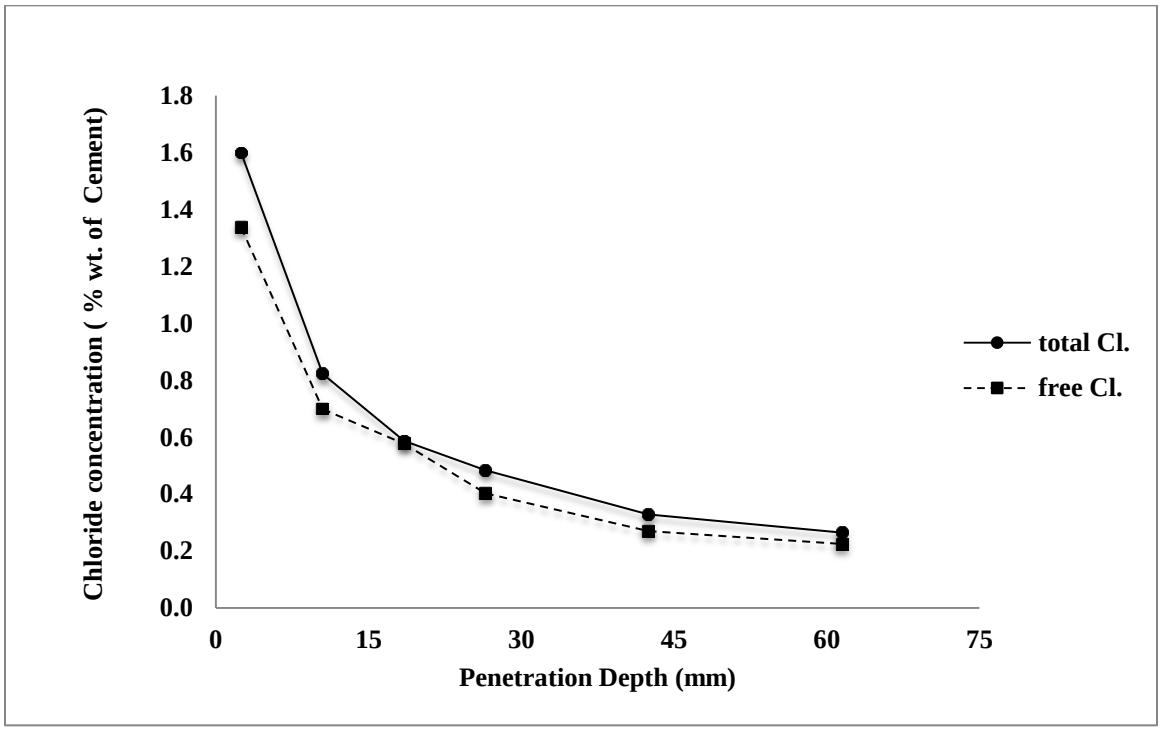

Figure 5.1: Free and Total chloride profile for M1-1D-T1

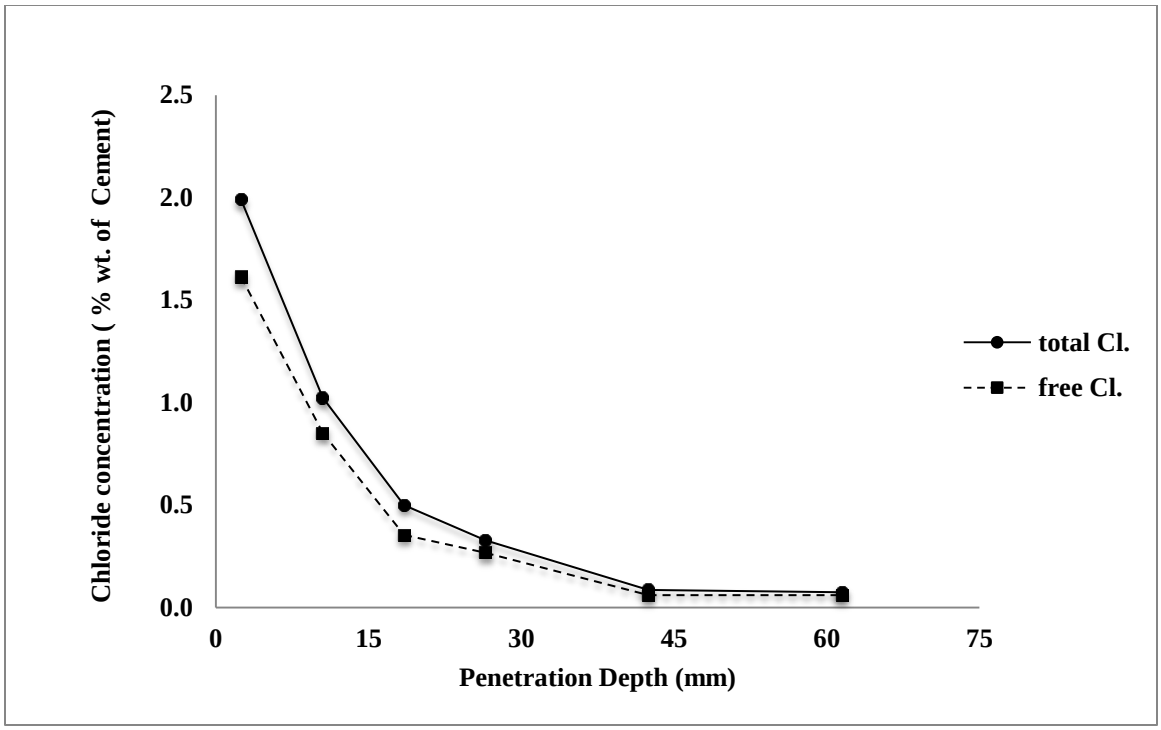

Figure 5.2: Free and Total chloride profile for M1-1D-T2

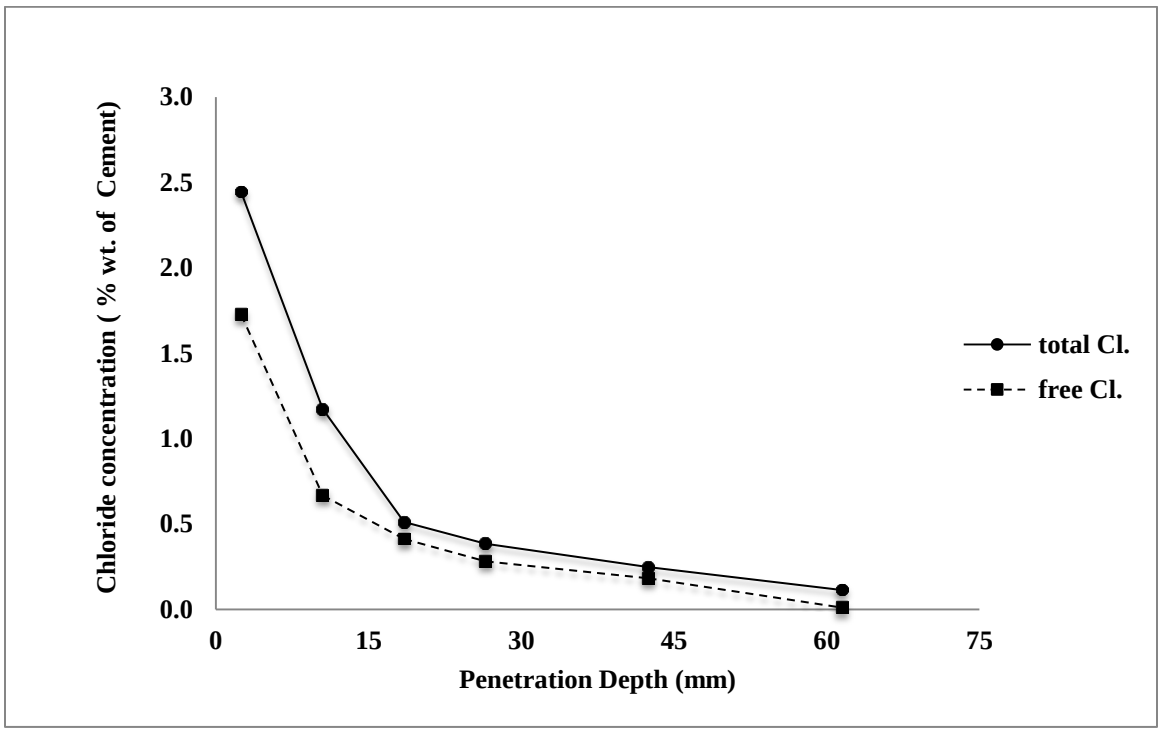

Figure 5.3: Free and Total chloride profile for M1-1D-T3

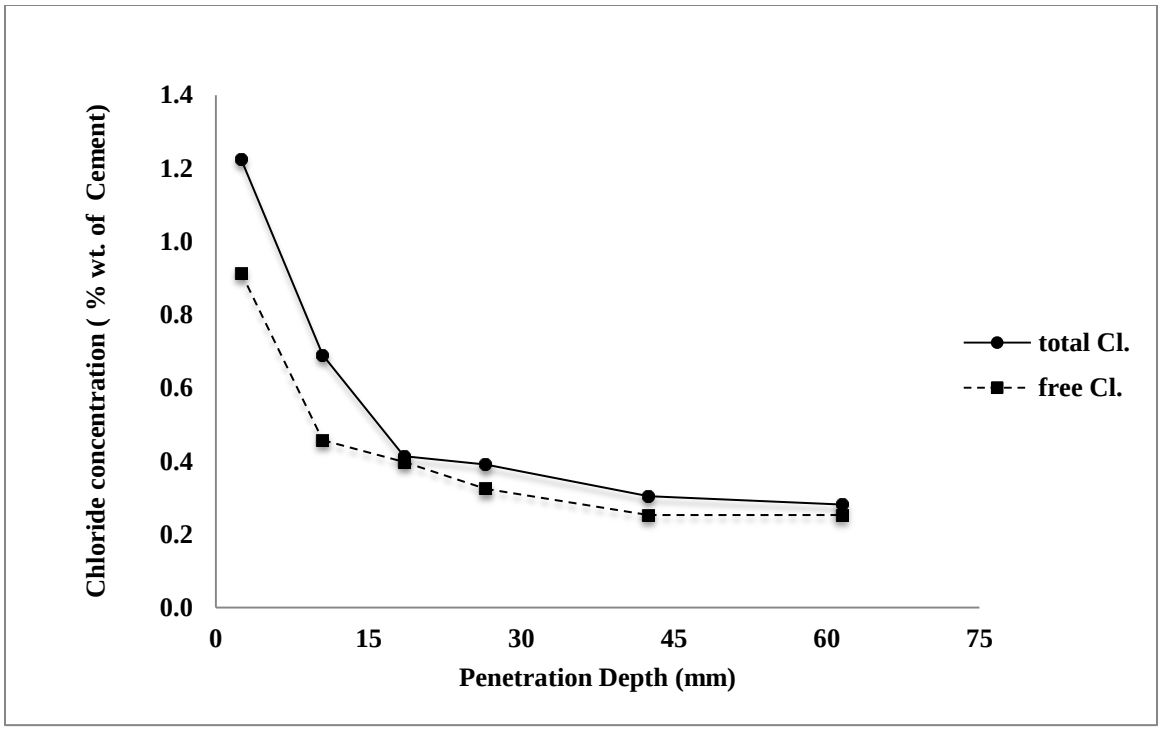

Figure 5.4: Free and Total chloride profile for M1-2D2-T1

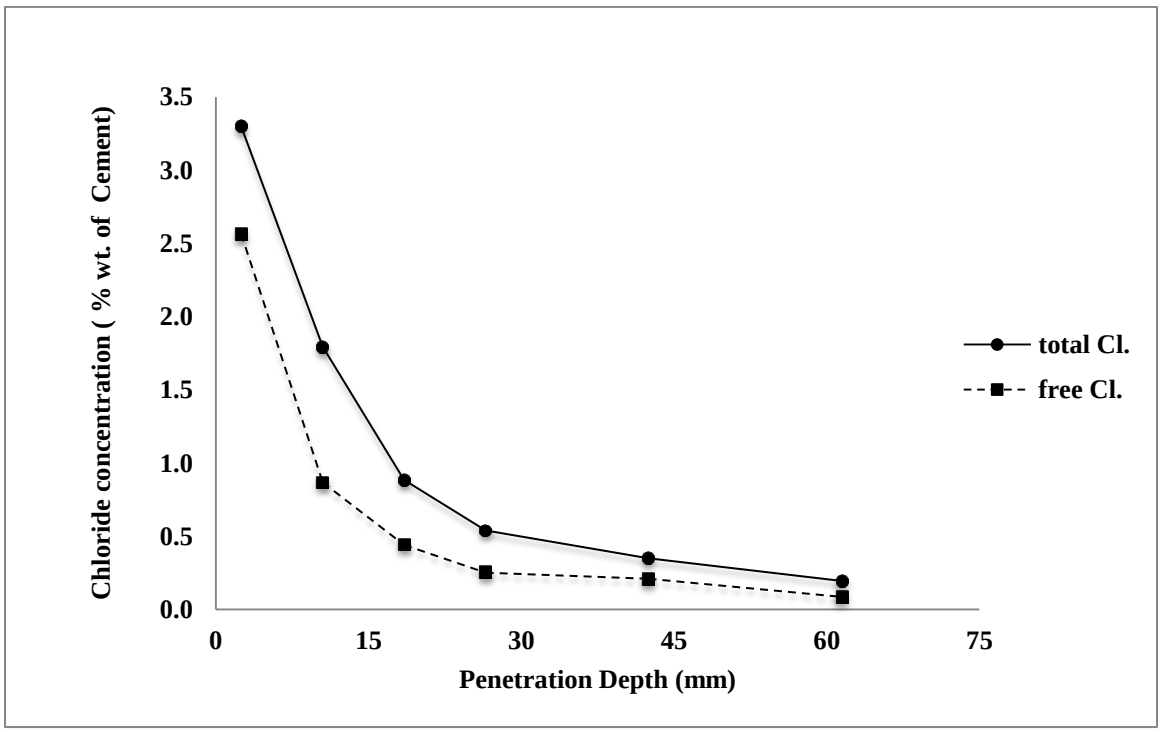

Figure 5.5: Free and Total chloride profile for M1-2D2-T2

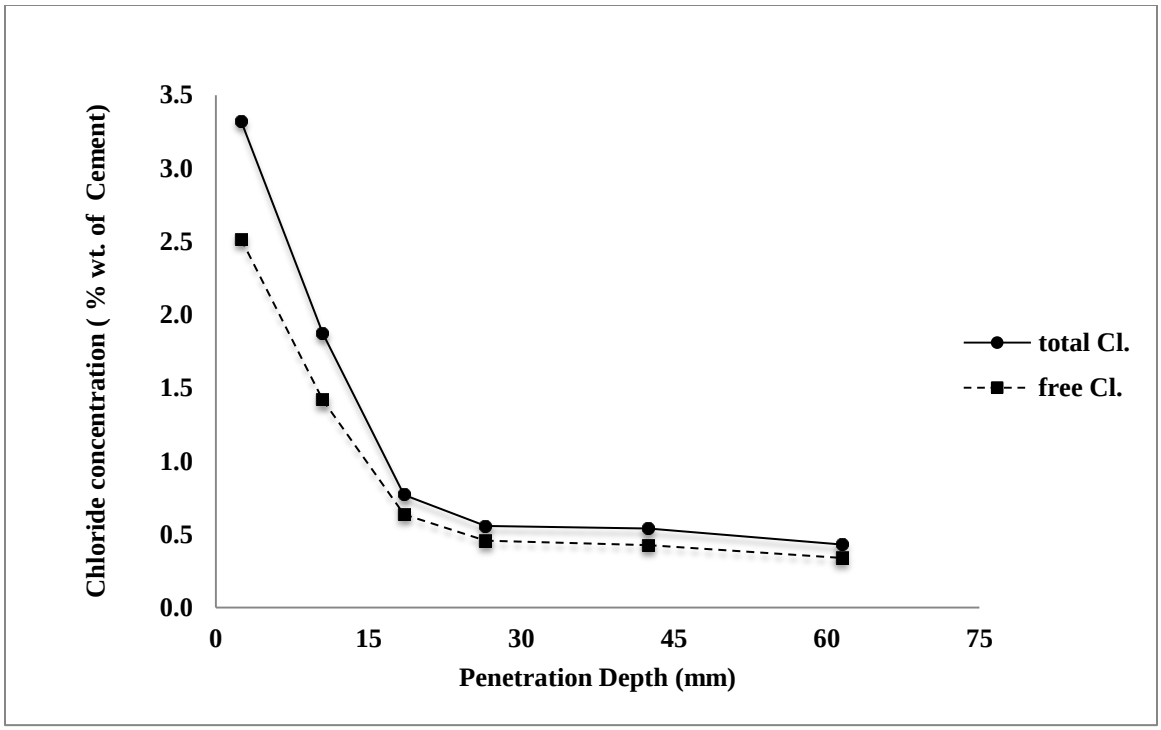

Figure 5.6: Free and Total chloride profile for M1-2D2-T3

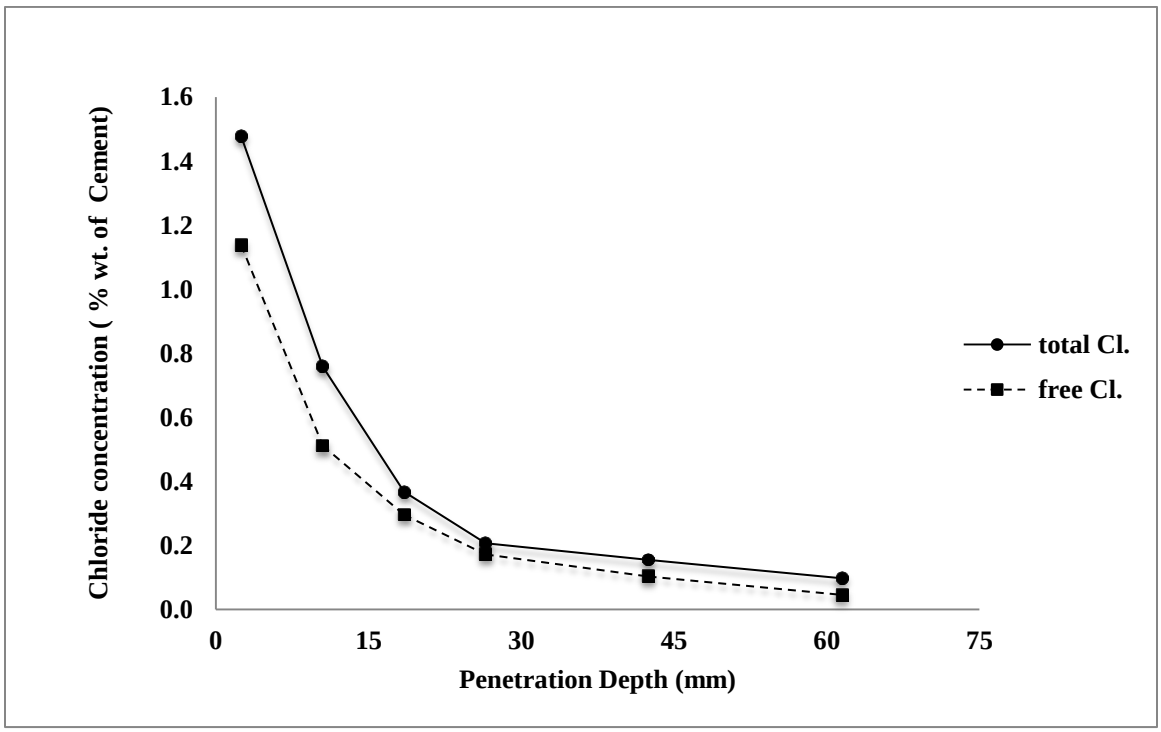

Figure 5.7: Free and Total chloride profile for M1-2D3-T1

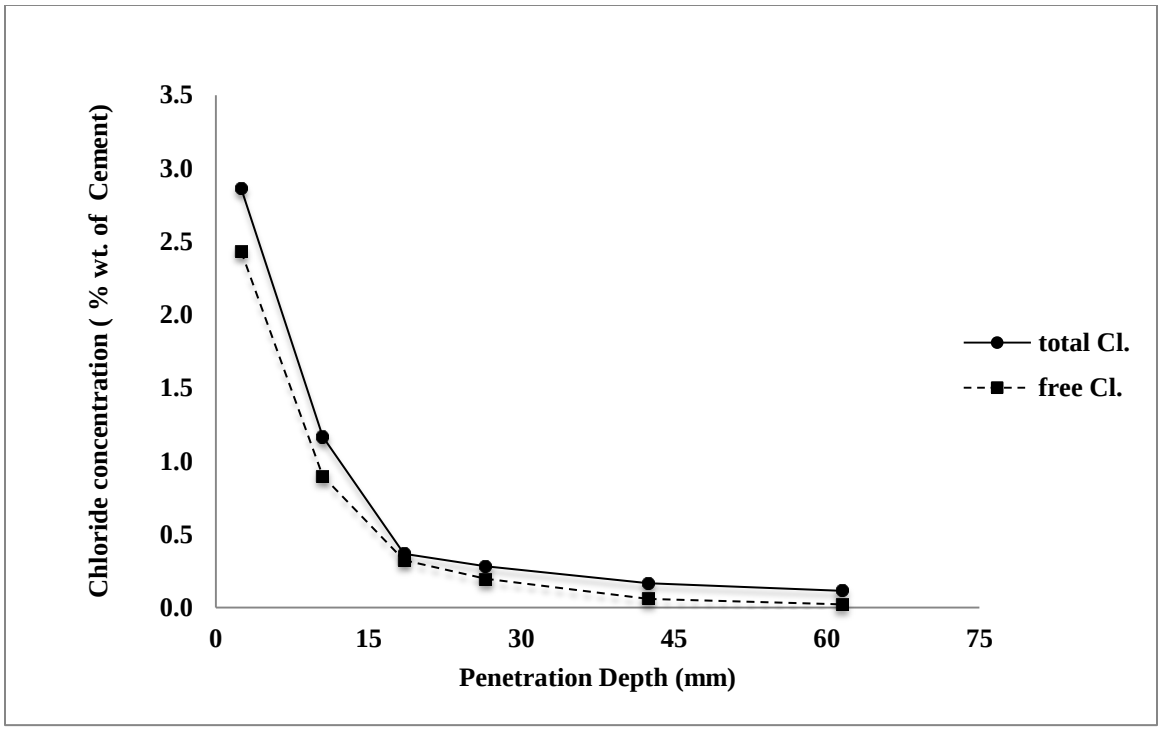

Figure 5.8: Free and Total chloride profile for M1-2D3-T2

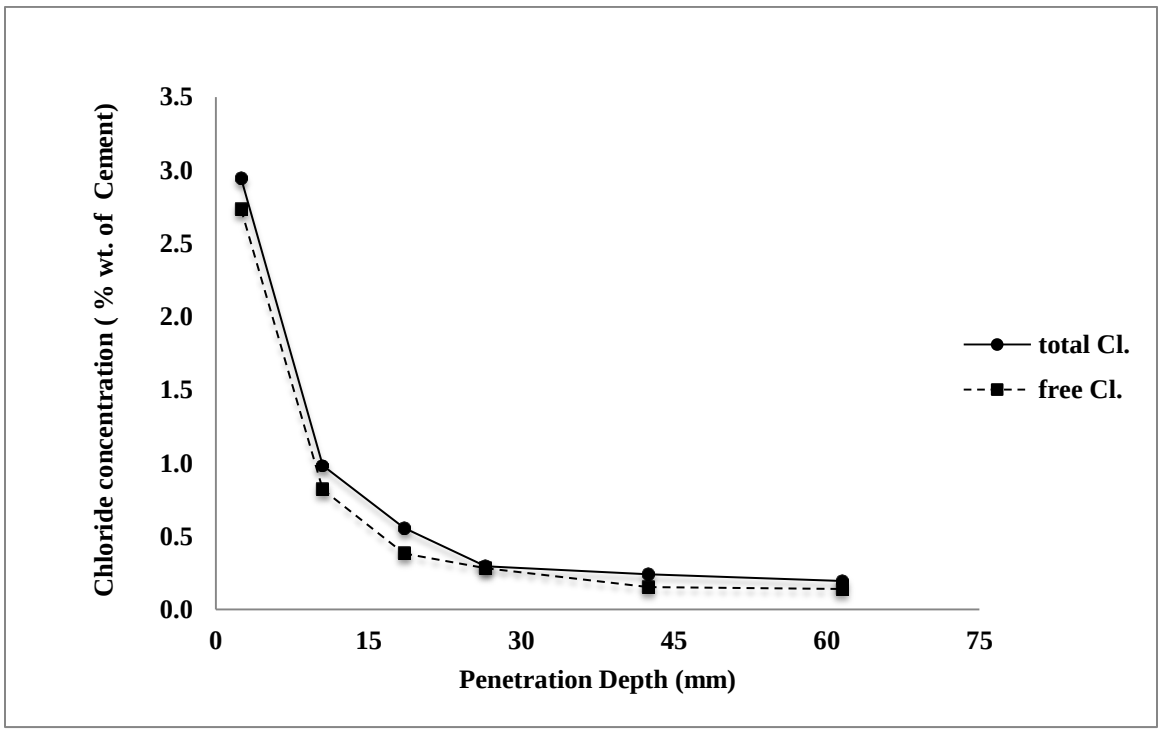

Figure 5.9: Free and Total chloride profile for M1-2D3-T3

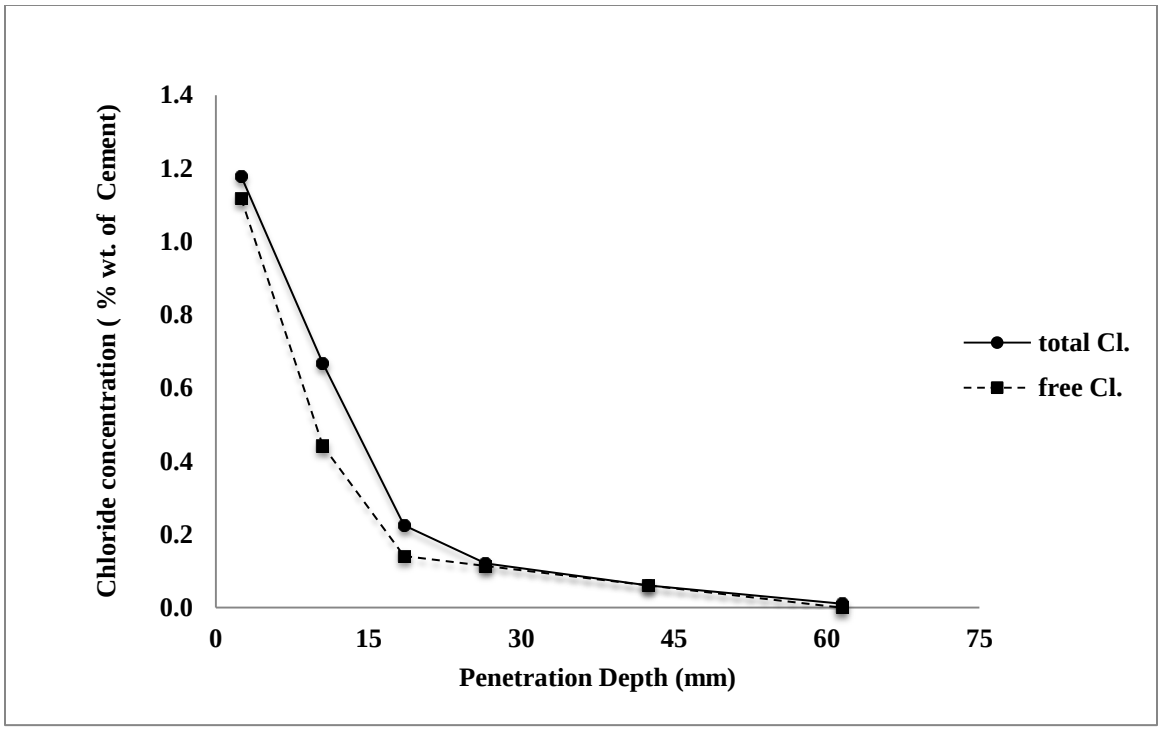

Figure 5.10: Free and Total chloride profile for M2-1D-T1

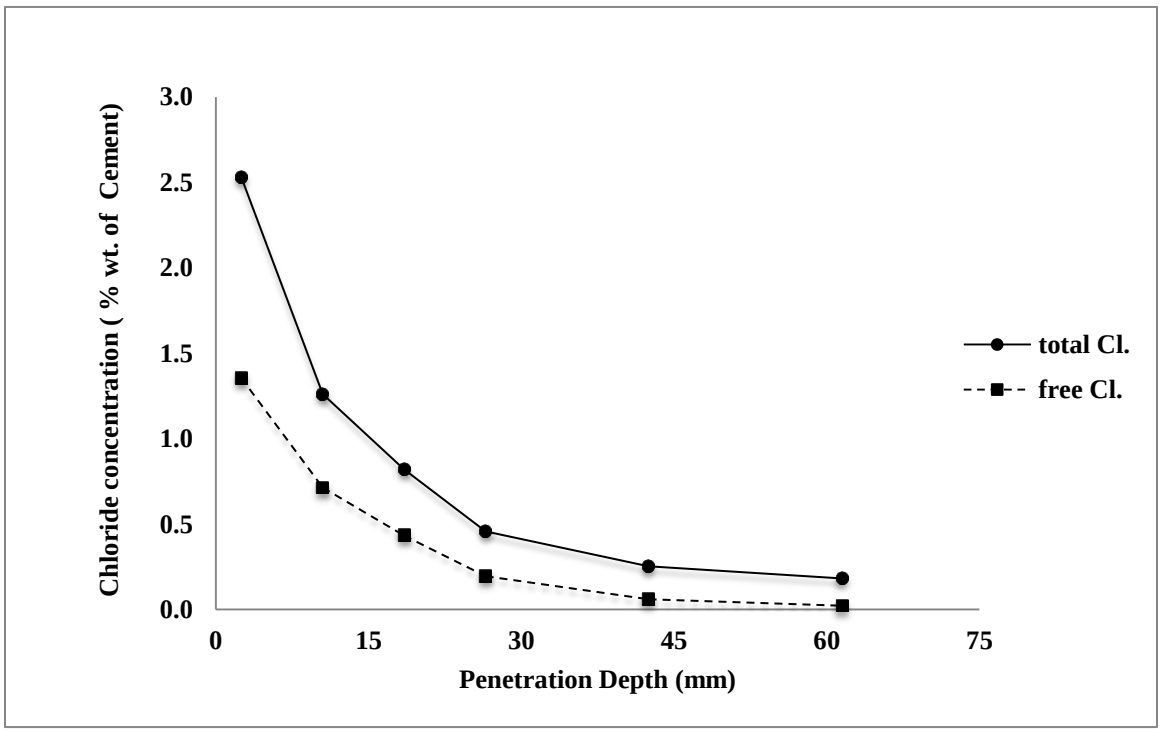

Figure 5.11: Free and Total chloride profile for M2-1D-T2

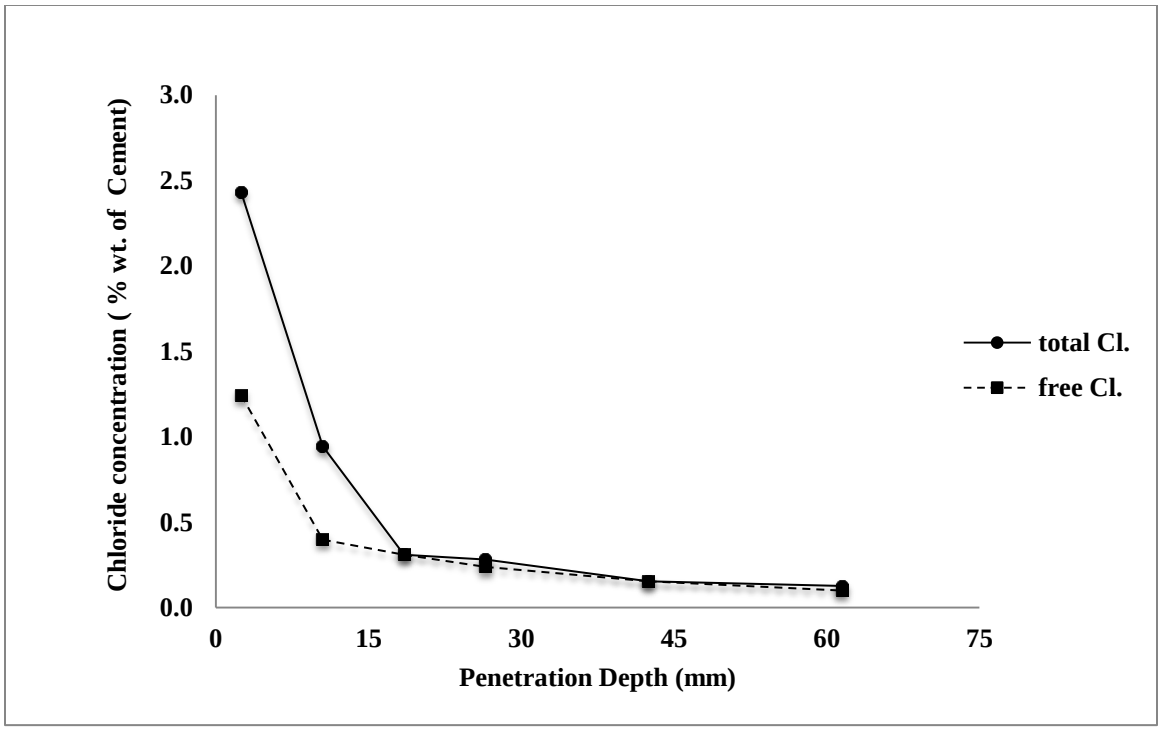

Figure 5.12: Free and Total chloride profile for M2-1D-T3

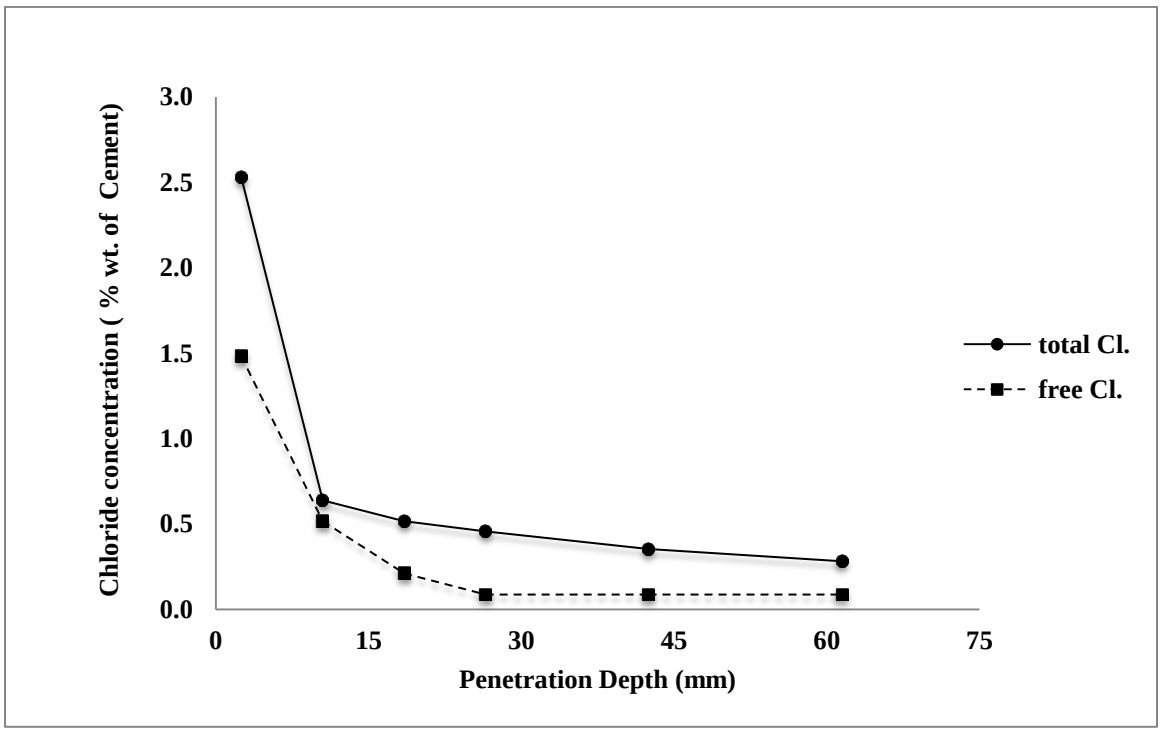

Figure 5.13: Free and Total chloride profile for M2-2D2-T1

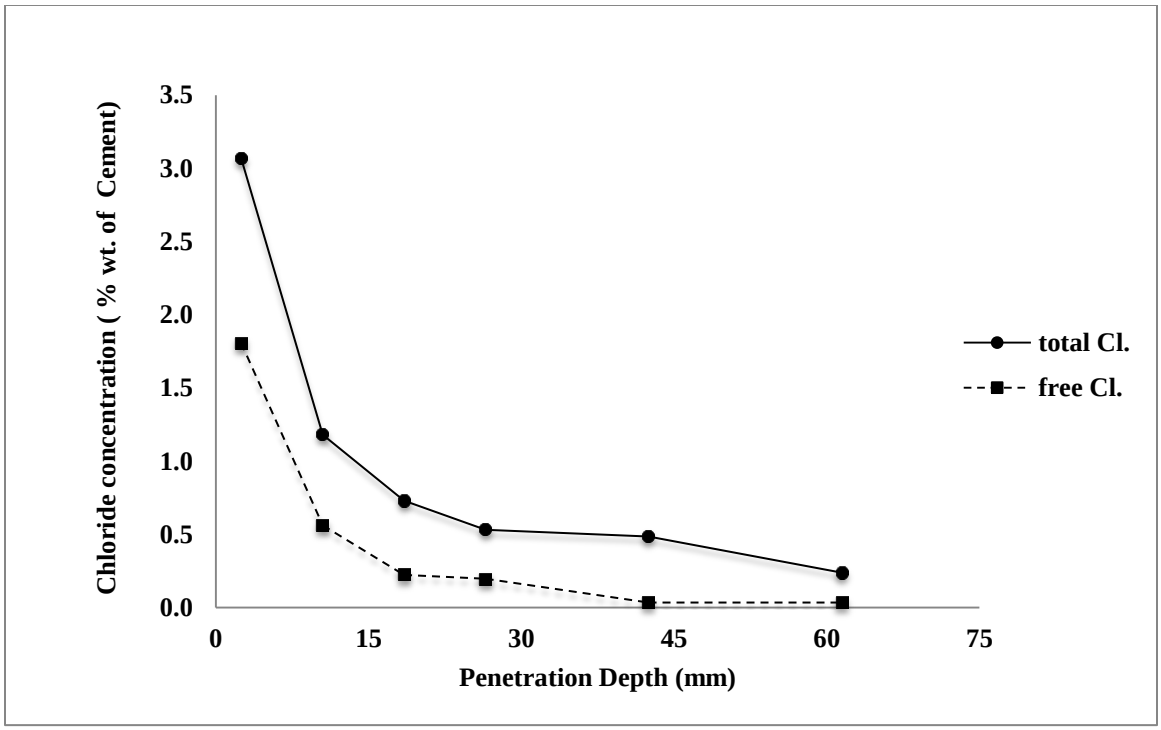

Figure 5.14: Free and Total chloride profile for M2-2D2-T2

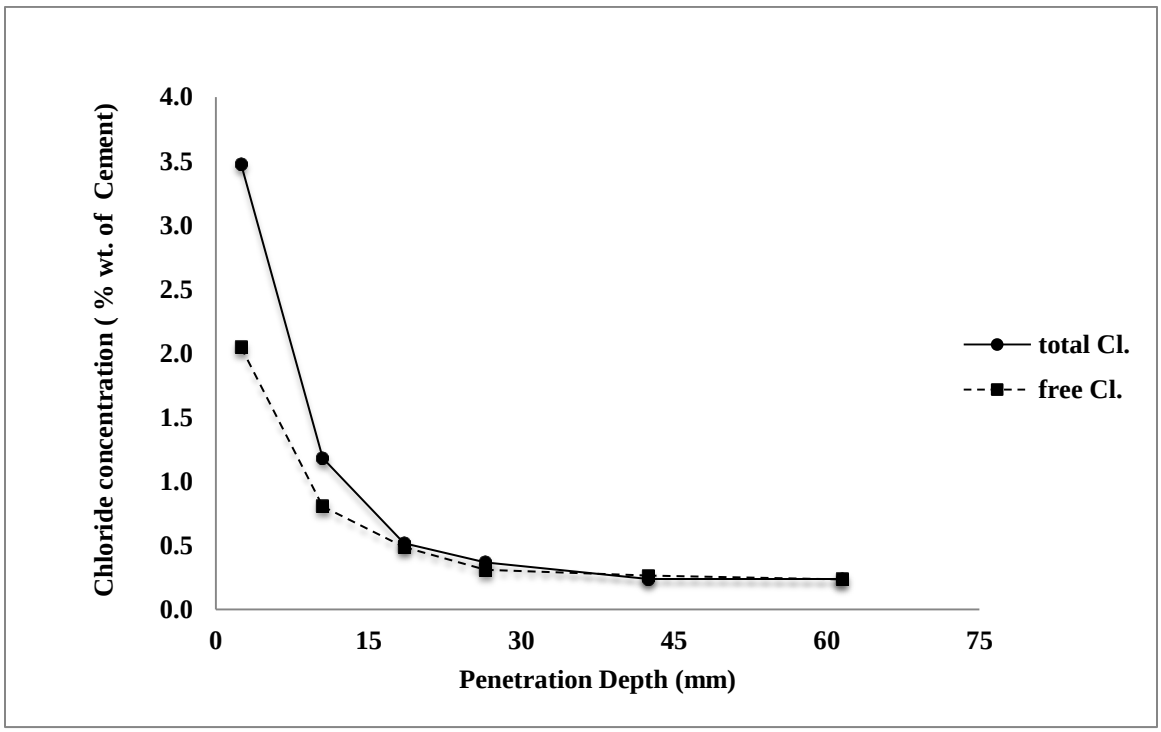

Figure 5.15: Free and Total chloride profile for M2-2D2-T3

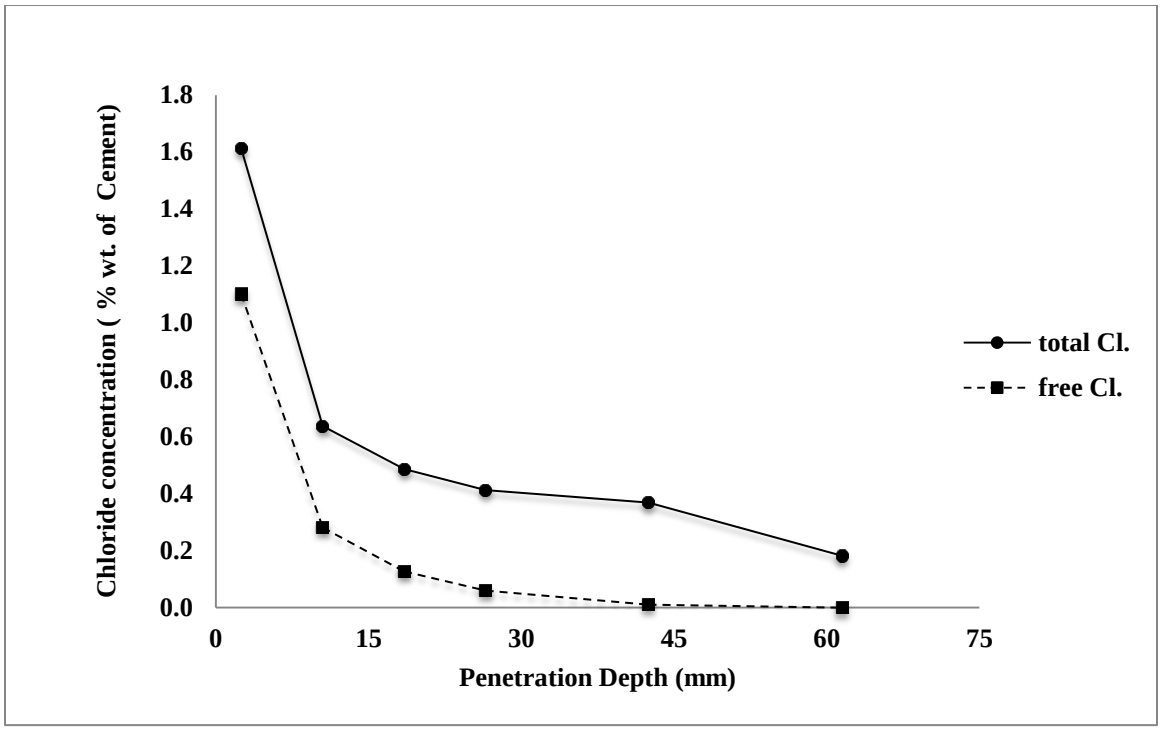

Figure 5.16: Free and Total chloride profile for M2-2D3-T1

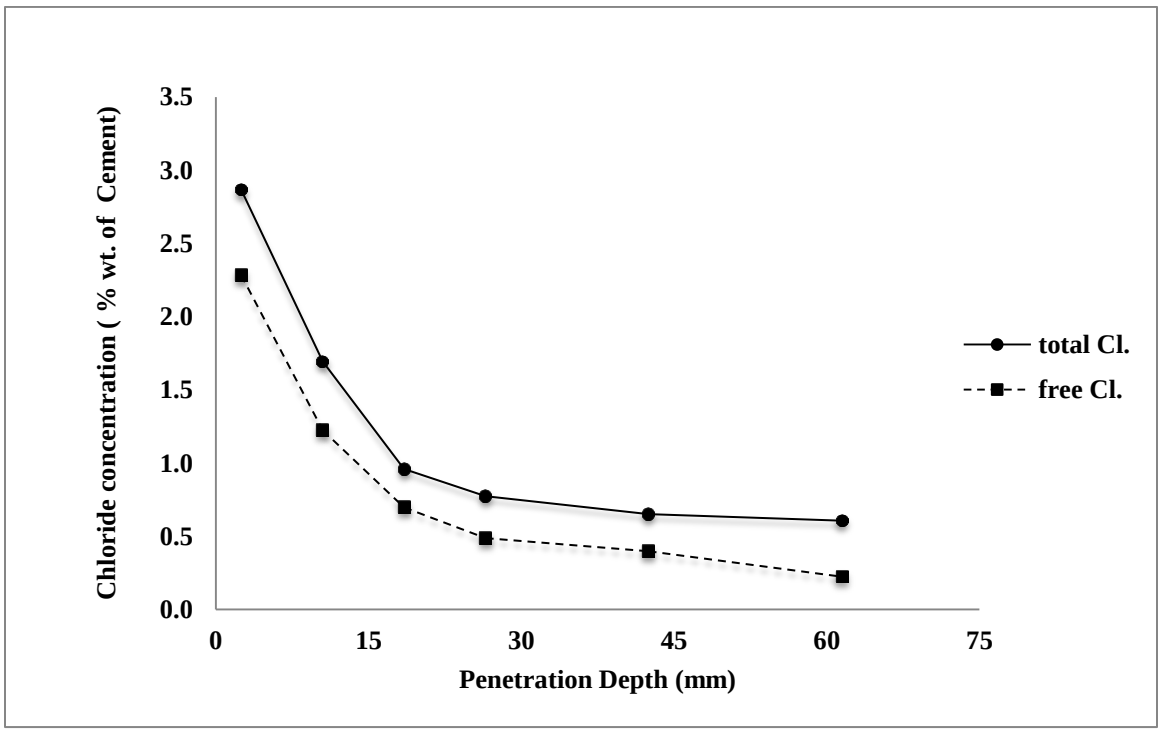

Figure 5.17: Free and Total chloride profile for M2-2D3-T2

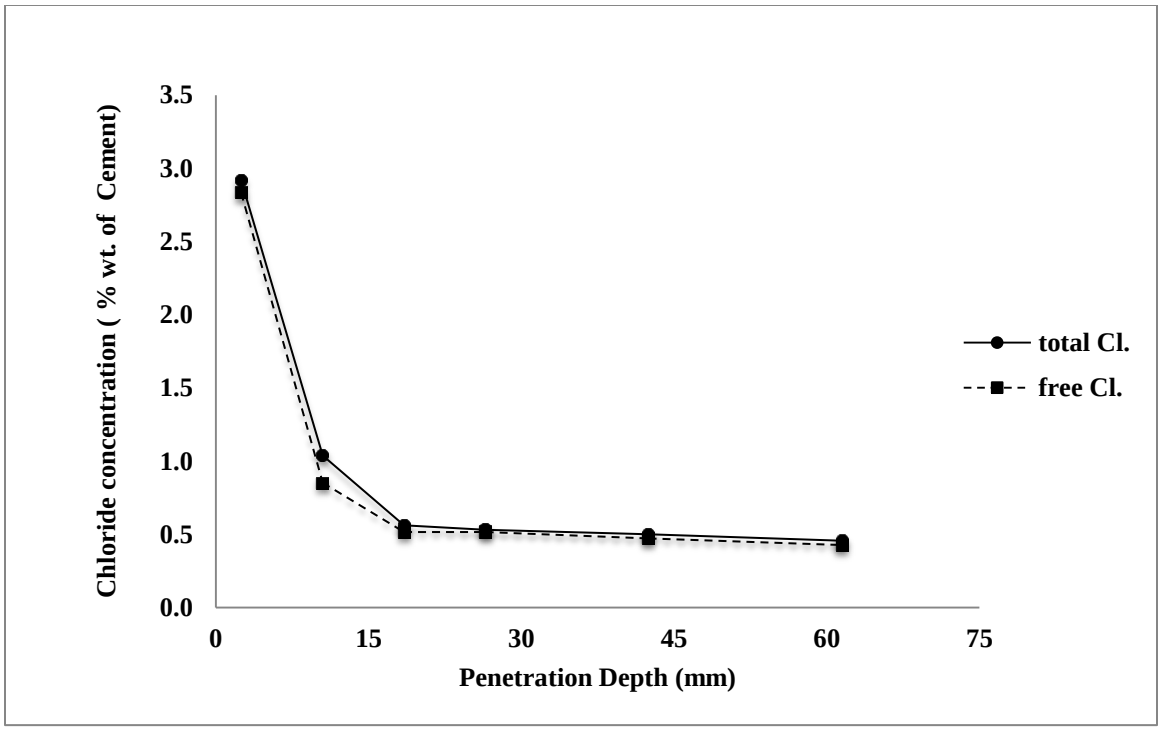

Figure 5.18: Free and Total chloride profile for M2-2D3-T3

5.3 Effect of Time on Chloride Diffusion Coefficient

Solution of Fick's 2nd law of Diffusion given by Crank (Model 1) assumes *D* as a constant. However, several researchers reported it to be decreasing with time [9]. Therefore, the chloride profiles were obtained at three exposure durations in order to analyze the effect of time on chloride diffusion coefficient. These values of *D* and C_s were obtained by fitting the Model 1 in Mathematica. Table 5.2 through Table 5.5 show the values of *D* and C_s evaluated at different exposure durations.

Table 5.2: Effect of time on *D* and C_s in Mix 1, 1-Direction exposure

Exposure (days)	Free Chloride		Total Chloride	
	***D* in 10^{-8} cm^2/sec**	**C_s**	***D* in 10^{-8} cm^2/sec**	**C_s**
50	83.52	1.28	71.02	1.54
120	11.08	1.83	11.70	2.23
165	6.62	1.93	7.27	2.76

Table 5.3: Effect of time on *D* and C_s in Mix 2, 1-Direction exposure

Exposure (days)	Free Chloride		Total Chloride	
	***D* in 10^{-8} cm^2/sec**	**C_s**	***D* in 10^{-8} cm^2/sec**	**C_s**
50	14.67	1.34	23.96	1.38
120	13.43	1.50	14.58	2.73
165	6.07	1.38	4.43	2.91

Table 5.4: Effect of time on *D* and C_s in Mix 1, 2-Direction exposure

Exposure (days)	Free Chloride		Total Chloride	
	***D* in 10^{-8} cm^2/sec**	**C_s**	***D* in 10^{-8} cm^2/sec**	**C_s**
50	189.89	1.86	187.78	2.28
120	15.02	5.65	26.06	7.33
165	9.21	5.39	8.39	7.44

Table 5.5: Effect of time on *D* and C_s in Mix 2, 2-Direction exposure

Exposure (days)	Free Chloride		Total Chloride	
	***D* in 10^{-8} cm^2/sec**	**C_s**	***D* in 10^{-8} cm^2/sec**	**C_s**
50	22.94	3.13	22.65	6.15
120	9.05	4.23	18.61	6.82
165	6.07	5.43	7.98	7.21

It is evident that the values for *D* were high at T1 and they reduced by one order upto T3 (83.52 x10^{-8} cm^2/sec at 50 days to 6.62 x10^{-8} cm^2/sec at 165 days). This can be attributed to the densification of microstructure with time. Similarly the C_s values showed an increasing trend with increase in time. This is due to the fact that, it is experimentally impossible to calculate the value of C_s; numerically the model is fitted with the data of chloride concentrations at different depths; which increases with time due to the ingress of external chloride ions, thus also increasing the value of C_s. Figure 5.19 and Figure 5.20 show the change in *D* with time.

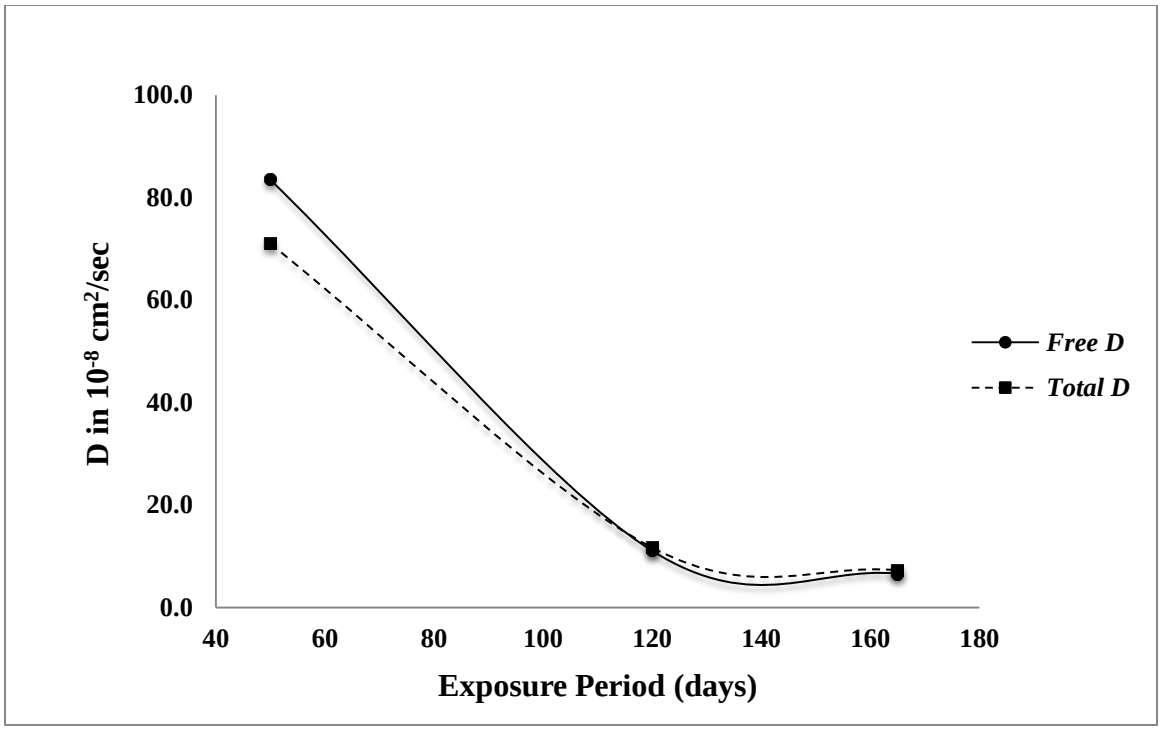

Figure 5.19: Effect of time on *D* in Mix 1, 1-Direction exposure

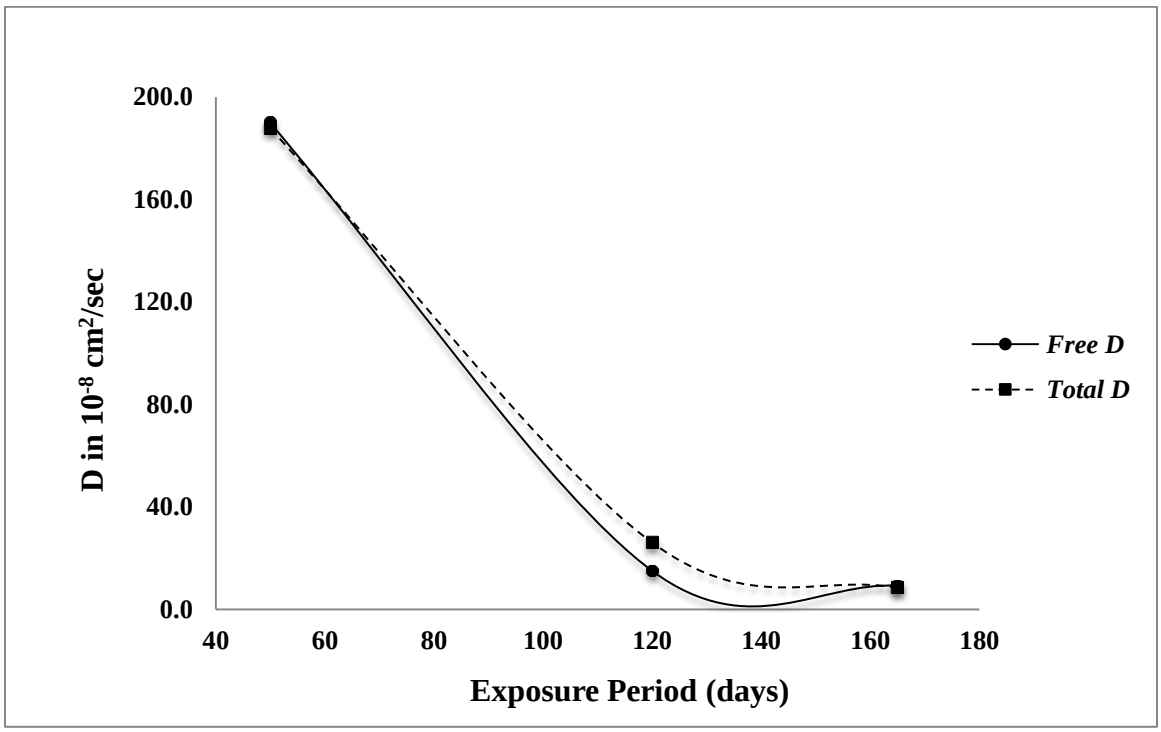

Figure 5.20: Effect of time on *D* in Mix 2, 1-Direction exposure

From Figure 5.19 and Figure 5.20, it can be observed that the time has significant effect on *D*, especially for the earlier durations of exposure, therefore it in necessary to account this change of *D* with time in chloride diffusion models. However, the decrease in *D* attenuates with the exposure duration. The methodology employed to capture this effect of time on *D* is explained in detail in Sec. 4.2.2 and a graphical demonstration is given in Figure 4.1. Moreover, it was also observed that the *free* and *total* chloride diffusivity values came out to be almost similar, although, these values were obtained from the different sets of data obtained from acid soluble and water soluble chloride analysis.

5.4 Chloride Binding Capacity

The external chloride diffusing into the concrete can be divided into two parts; free chloride and Total chloride. In Sec. 5.2 it is already discussed that some part of the chloride diffusing from outside binds chemically with C_3A and C-S-H gel to form Friedel's salt. Moreover some of the chloride ions physically adsorb within the microstructure of concrete.

These chloride binding capacities are expressed with respect to total chloride concentrations. Formula for calculating chloride binding capacity is given in Eq. 5.1:

$$\text{Chloride Binding Capacity} = \left\{ \frac{(\text{total chloride} - \text{free chloride})}{\text{toatal chloride}} * 100 \right\} \% \qquad \text{(Eq. 5.1)}$$

From the values of chloride capacity along the depth, as presented in Table 5.6 through Table 5.11, it was observed that the chloride binding capacity of the concrete changes with depth and quality of concrete mixture.

Table 5.6: Chloride Binding Capacity of M1-1D-T1

Depth (mm)	Total Chloride (% wt. of Cement)	Free Chloride (% wt. of Cement)	Bound Chloride (% wt. of Cement)	Binding Capacity (%)
2.5	1.599	1.337	0.262	16.370
10.5	0.822	0.698	0.124	15.053
18.5	0.587	0.577	0.009	1.617
26.5	0.483	0.402	0.081	16.680
42.5	0.328	0.270	0.058	17.761
61.5	0.265	0.225	0.040	15.079

Table 5.7: Chloride Binding Capacity of M1-1D-T2

Depth (mm)	Total Chloride (% wt. of Cement)	Free Chloride (% wt. of Cement)	Bound Chloride (% wt. of Cement)	Binding Capacity (%)
2.5	1.990	1.613	0.376	18.920
10.5	1.024	0.852	0.171	16.727
18.5	0.500	0.354	0.146	29.204
26.5	0.328	0.267	0.060	18.428
42.5	0.086	0.061	0.026	29.839
61.5	0.075	0.061	0.014	19.045

Table 5.8: Chloride Binding Capacity of M1-1D-T3

Depth (mm)	Total Chloride (% wt. of Cement)	Free Chloride (% wt. of Cement)	Bound Chloride (% wt. of Cement)	Binding Capacity (%)
2.5	2.444	1.726	0.717	29.352
10.5	1.173	0.668	0.505	43.055
18.5	0.512	0.413	0.099	19.324
26.5	0.385	0.282	0.104	26.878
42.5	0.247	0.182	0.065	26.220
61.5	0.114	0.011	0.103	90.508

Table 5.9: Chloride Binding Capacity of M2-1D-T1

Depth (mm)	Total Chloride (% wt. of Cement)	Free Chloride (% wt. of Cement)	Bound Chloride (% wt. of Cement)	Binding Capacity (%)
2.5	1.179	1.118	0.061	5.155
10.5	0.668	0.442	0.226	33.766
18.5	0.225	0.141	0.084	37.283
26.5	0.121	0.114	0.007	5.910
42.5	0.061	0.061	0.000	0.000
61.5	0.011	0.000	0.011	100.000

Table 5.10: Chloride Binding Capacity of M2-1D-T2

M2-1D-T2				
Depth (mm)	**Total Chloride (% wt. of Cement)**	**Free Chloride (% wt. of Cement)**	**Bound Chloride (% wt. of Cement)**	**Binding Capacity (%)**
2.5	2.533	1.356	1.177	46.457
10.5	1.260	0.714	0.547	43.372
18.5	0.821	0.434	0.388	47.216
26.5	0.457	0.196	0.261	57.044
42.5	0.253	0.061	0.193	76.086
61.5	0.182	0.023	0.160	87.575

Table 5.11: Chloride Binding Capacity of M2-1D-T3

M2-1D-T3				
Depth (mm)	**Total Chloride (% wt. of Cement)**	**Free Chloride (% wt. of Cement)**	**Bound Chloride (% wt. of Cement)**	**Binding Capacity (%)**
2.5	2.433	1.245	1.188	48.843
10.5	0.946	0.398	0.547	57.893
18.5	0.311	0.311	0.000	0.000
26.5	0.282	0.239	0.043	15.228
42.5	0.155	0.155	0.000	0.000
61.5	0.127	0.100	0.027	21.270

From the values of % chloride binding presented in Table 5.6 through Table 5.11, it is evident that the chloride binding capacities are changing over the course of time and concrete mixture, M2, showed higher binding capacities than M1 (on average 38% for M2 v/s 25% for M1). The greater amount of chloride binding in Silica fume concrete

(M2) can be attributed to the fact that, due to the dense microstructure a greater amount of chloride will be intercepted.

5.5 Service life prediction

Service life of reinforced concrete structure can be divided into two parts:

1. Time for corrosion initiation
2. Time for corrosion propagation

Tuutti [11] presented the

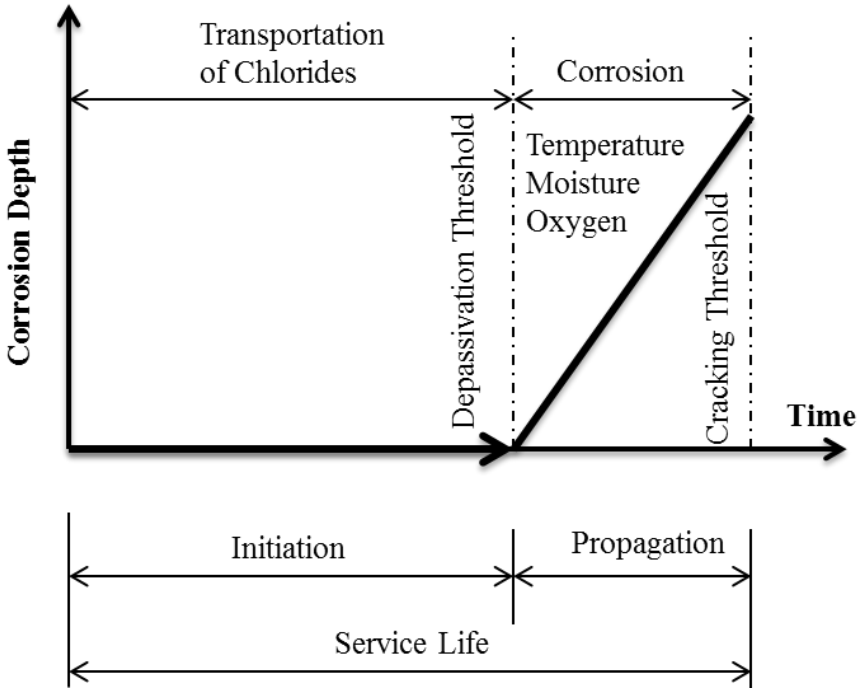

Figure 5.21; that elaborates this idea:

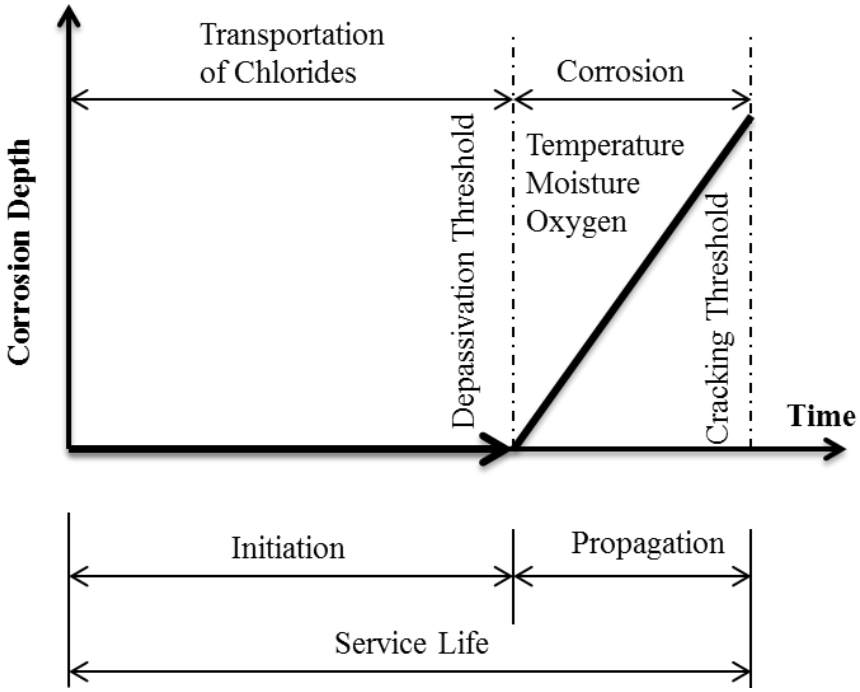

Figure 5.21: Conceptual Corrosion Sequence in Concrete (Tuutti, 1982)

In this study only the first part of the service life is considered; i.e. time in which threshold chloride concentration is attained at the rebar level. International codes specify different threshold chloride concentrations. ACI code is followed in this study for the calculation of time for corrosion initiation. The limits specified by the ACI code are given in the Table 5.12:

Table 5.12: ACI Code Chloride Limits for New Construction

Construction type and condition	Chloride limit, percent by mass		
	Test method		
	Acid soluble	Water soluble	
	ASTM C1152	ASTM C1218	Soxhlet*
Prestressed concrete	0.08	0.06	0.06
Reinforced concrete wet in service	0.10	0.08	0.08
Reinforced concrete dry in service	0.20	0.15	0.15
*The Soxhlet test method is described in ACI 222.1.[4.8]			

Following threshold limits were adopted for the calculation of time of onset of corrosion:

- 0.15% by weight of cement for free chloride (water soluble) concentration.
- 0.2% by weight of cement for total chloride (acid soluble) concentration.

For clarity of presentation, service life prediction is divided into the following sub-sections:

1. Comparison of all Models in terms of service life prediction
2. Comparison of service life prediction by free chloride and total chloride threshold concentration

5.5.1 Comparison of all Models in terms of service life prediction

The values of time of initiation of corrosion were computed with respect to total chloride threshold concentration i.e. 0.2 % by wt. of cementitious material. Figure 5.22 and Figure 5.23 show the comparison of all 5 Models for different exposure conditions:

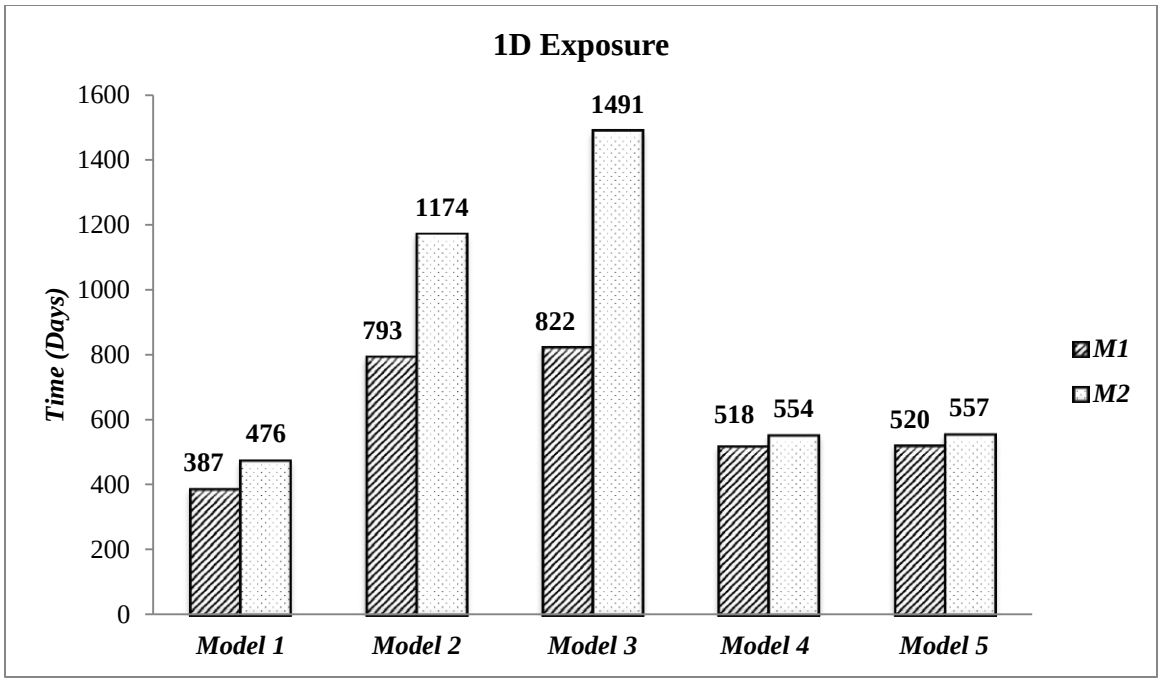

Figure 5.22: Comparison of Service Life between M1 and M2 for 1D exposure

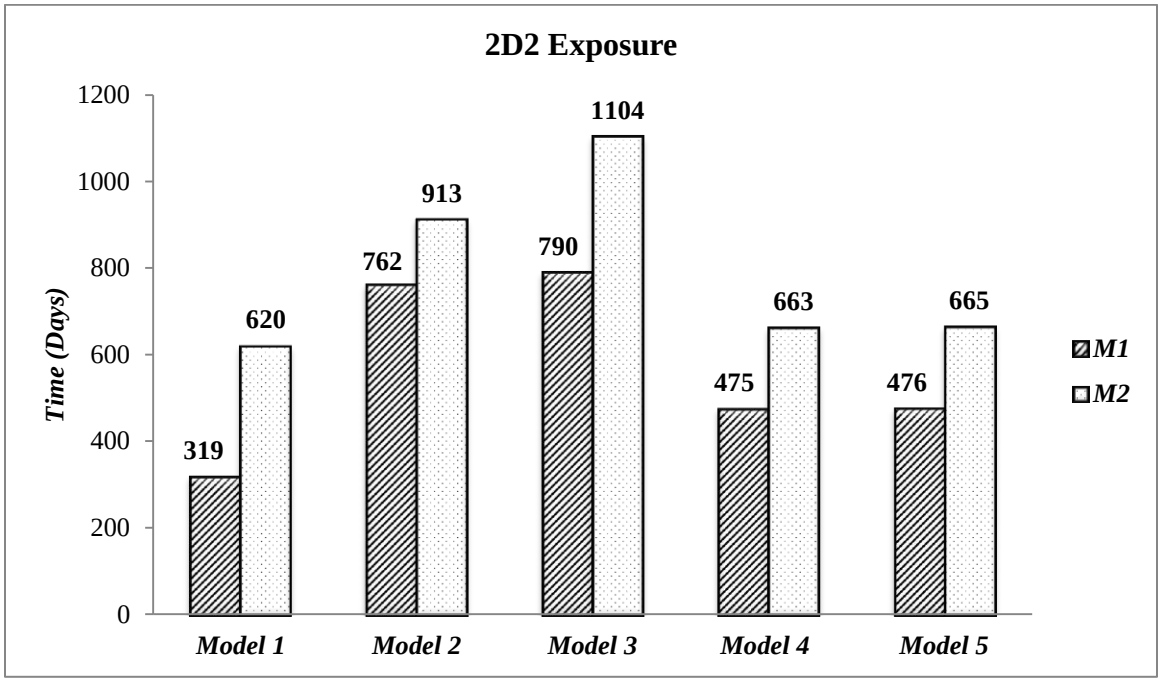

Figure 5.23: Comparison of Service Life between M1 and M2 for 2D2 exposure

In all exposure conditions the service life predicted for M2 is greater than M1. This is consistent because the Silica fume improves the mechanical and durability properties by

enhancing the microstructure of concrete. Comparing between models; it was observed that Model 1 predicted the smallest values of service life, because it does not consider the effects of change in chloride diffusion coefficient with time and binding between chloride ions and hydration products.

Service life predicted by Model 2 was significantly more than Model 1; because of consideration of change in chloride diffusion coefficient with time. It was observed that, neglecting the effect of time on chloride diffusion coefficient will result in underestimation of concrete durability properties.

Model 3 predicted the highest values of service life, because, it also considers the effect of binding between chloride ions and hydration products along with the effect of time on chloride diffusion coefficient. However, if the experimental data of free chloride concentration is available only, then Model 3 shrinks to Model 2. This is because of the chloride binding term "*k*" becomes zero. Moreover, it was observed that the difference between the predicted service life values of Models 2 and 3 was relatively much less than the difference between the values of Models 1 and 2. Therefore it can be concluded that the effect of change in diffusion coefficient with time is more prominent than chloride binding.

Models 4 and 5 predicted almost the similar values of time of onset of corrosion. These values were more than Model 1 but less than the predicted values of Models 2 and 3. This is because of the reason that, Models 4 and 5 only considers the effect of chloride binding and the effect of change in chloride diffusion coefficient is not counted.

5.5.2 Comparison of service life prediction by free chloride and total chloride threshold concentration and effect of taking D as a function of time

ACI code specifies the threshold limits for both free and total chloride concentrations. Values of threshold chloride concentration are given in Table 5.12. Service life is predicted from both of the threshold limits and the comparison is shown in Figure 5.24 and Figure 5.25:

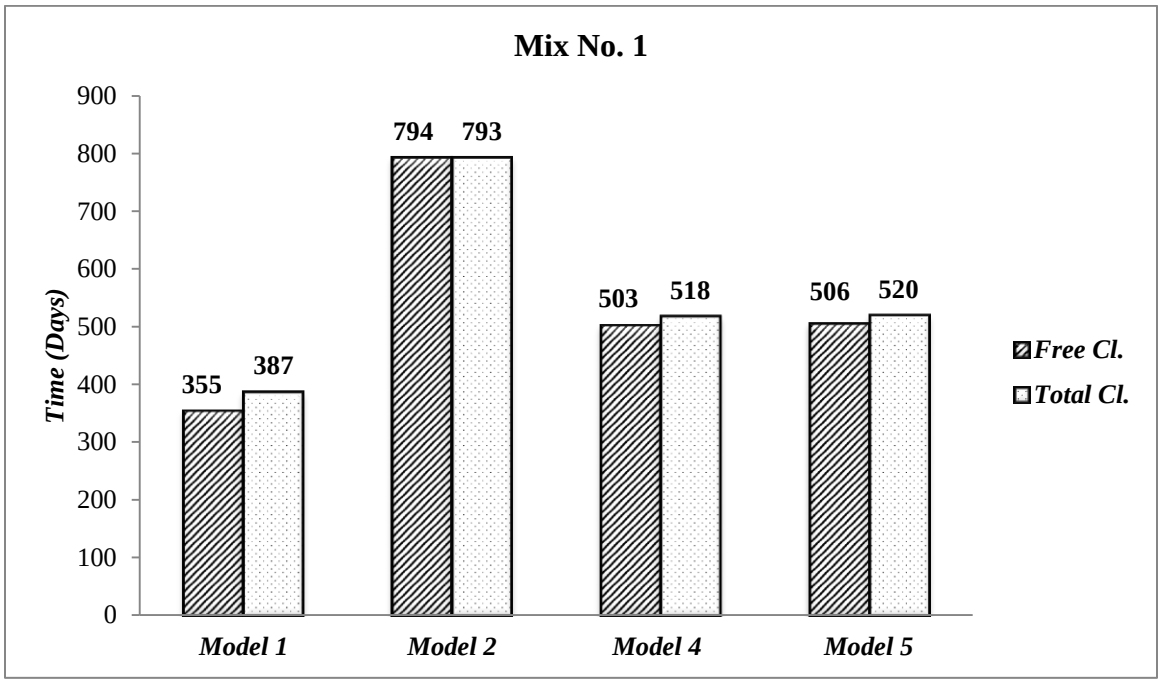

Figure 5.24: Comparison of Service Lives calculated by Free and Total Chloride threshold limits for Mix 1

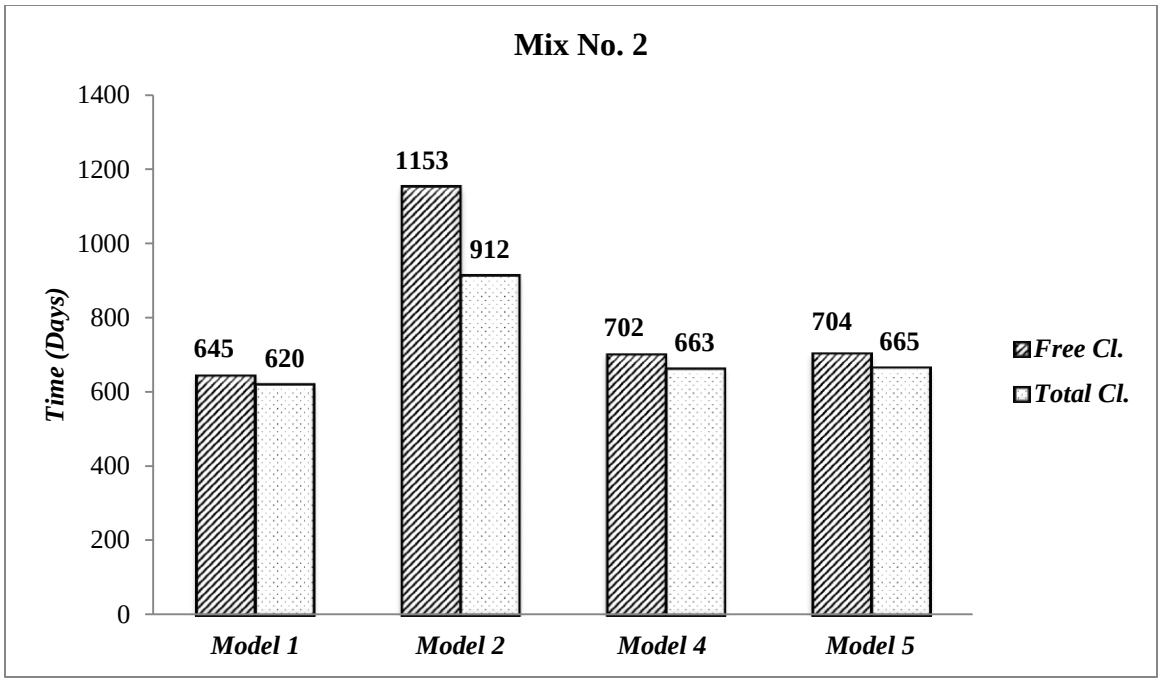

Figure 5.25: Comparison of Service Lives calculated by Free and Total Chloride threshold limits for Mix 2

It can be observed from the Figure 5.24 and Figure 5.25 that both the limits set by ACI yielded almost the similar service lives. Therefore, it can be concluded that the limits prescribed by ACI are well in proportion for catering the effect of chloride binding. It is to be noted that the values of service lives of Model 3 are not presented in Figure 5.24 and Figure 5.25, because the Model 3 shrinks to Model 2 in case of free chloride concentration data due to "*k*" becomes zero in Model 3.

CHAPTER 6

CONCLUSIONS

6.1 Conclusions

An effort was made in this work to study the dependence of chloride diffusion on time, chloride binding, and multi-directional ingress of chloride, which is normally not addressed by the models based on Fick's 2nd Law of diffusion. Results have shown the significant effects of these factors on chloride diffusion coefficient and therefore on time of initiation of reinforcement corrosion.

Based on the outcomes of this study following conclusions can be drawn:

1. Chloride profiles plotted using the experimental data show that the total chloride concentration is always greater than free chloride concentration, confirming the effect of chloride binding in concrete. This binding effect was found to be more prominent in silica fume concrete than OPC concrete due to the denser microstructure of the silica fume concrete.
2. Chloride diffusion coefficient was found to decrease significantly with time due to the densification of concrete microstructure. A sharp decrease in the chloride diffusion coefficient was observed during the earlier exposure durations due to the faster rate of hydration reactions.
3. Besides calculating chloride diffusion coefficient, the experimental data was utilized to determine corrosion initiation time using a set of five alternate models. Comparison of the results obtained using different models enabled to examine the effects of various factors considered in the study.

4. The values of time to initiation of reinforcement corrosion calculated using threshold chloride concentration set by ACI either in terms of free chloride or total chloride came out to be almost similar. This confirms the adequacy of the both limits set by the ACI.
5. A chloride diffusion model (3^{rd} Model) was proposed along with the approach for solving it numerically incorporating the effects of time and chloride binding. The accuracy of this model in calculating the chloride diffusion coefficient and corrosion initiation time was compared with that of the other alternate models. It was observed that the proposed model captured the interaction effect of chloride diffusion due to multi-directional exposure besides capturing the effects of time and chloride binding. Therefore, the proposed model can be used in service life prediction against chloride-induced corrosion with more degree of accuracy.

REFERENCES

[1] M. H. Baluch, M. Asce, M. K. Rahman, and A. H. Al-gadhib, "Risks of Cracking and Delamination in Patch Repair," vol. 285, no. AUGUST, pp. 294–302, 2002.

[2] M. G. Alexander, M. Santhanam, and Y. Ballim, "Durability design and specification for concrete structures—the way forward," *Int. J. Adv. Eng. Sci. Appl. Math.*, vol. 2, no. 3, pp. 95–105, Mar. 2011.

[3] W. A. S. Al-Kutti, "Simulation of Chloride Transport in Concrete with Stress induced Damage," 2011.

[4] L.-Y. Li, J. Xia, and S.-S. Lin, "A multi-phase model for predicting the effective diffusion coefficient of chlorides in concrete," *Constr. Build. Mater.*, vol. 26, no. 1, pp. 295–301, Jan. 2012.

[5] G. J. Verbeck, "Mechanisms of corrosion in Concrete," in *Corrosion of metals in concrete*, 1975, pp. 21–38.

[6] E. J. Garboczi, "(Commtmieated by R.E. Philleo) (Received Sept 25, 1989)," vol. 20, pp. 591–601, 1990.

[7] A. Naville, "Chloride Attack," in *Properties of concrete*, 1996, pp. 563–75.

[8] B. Martõ, "A study of the effect of chloride binding on service life predictions," vol. 30, pp. 1215–1223, 2000.

[9] Y.-M. Sun, M.-T. Liang, and T.-P. Chang, "Time/depth dependent diffusion and chemical reaction model of chloride transportation in concrete," *Appl. Math. Model.*, vol. 36, no. 3, pp. 1114–1122, Mar. 2012.

[10] S.-H. Han, "Influence of diffusion coefficient on chloride ion penetration of concrete structure," *Constr. Build. Mater.*, vol. 21, no. 2, pp. 370–378, Feb. 2007.

[11] K. TUUTTI, "CORROSION OF STEEL IN CONCRETE," *Cem. Concr. Res.*, no. 4, p. 468, 1982.

[12] H. L. -O. Nilsson, E. Poulsen, P. Sandberg, H.E. Sùrensen, O. Klinghoffer, "Chloride penetration into concrete, State - of - the - art, Transport Processes, Corrosion Initiation, Test Methods and Penetration Models," 1996.

[13] G. K. Glass and N. R. Buenfeld, “The influence of chloride binding on the chloride induced corrosion risk in reinforced concrete,” vol. 42, pp. 329–344, 2000.

[14] Q. Yuan, C. Shi, G. De Schutter, K. Audenaert, and D. Deng, “Chloride binding of cement-based materials subjected to external chloride environment – A review,” *Constr. Build. Mater.*, vol. 23, no. 1, pp. 1–13, Jan. 2009.

[15] J. Maage, M; Helland, S; Poulsen, E; Vennesland, O; Carlsen, “Service life prediction of existing concrete structures exposed to marine environment,” *ACI Mater. J.*, vol. 93, pp. 602 – 608, 1996.

[16] B. Elsener and U. Angst, “Mechanism of electrochemical chloride removal,” *Corros. Sci.*, vol. 49, no. 12, pp. 4504–4522, Dec. 2007.

[17] M. Collepardi, “Quick Method to Determine Free and Bound Chlorides in Concrete,” in *RILEM*, 1995, pp. 10–16.

[18] M. P. F., “Development of test methods for predicting chloride penetration into high performance concrete,” University of Toronto, Canada., 1996.

[19] G. K. GLASS, N. M. HASSANEIN, and N. R. Buenfeld, “NEURAL NETWORK MODELLING OF CHLORIDE BINDING,” *Mag. Concr. Res.*, vol. 49, no. 181, p. P 323–35.

[20] P. P. Lid and R. March, “OPC paste,” vol. 23, no. 2, pp. 247–253, 1993.

[21] M. Nokken, A. Boddy, R. D. Hooton, and M. D. a. Thomas, “Time dependent diffusion in concrete—Three laboratory studies,” *Cem. Concr. Res.*, vol. 36, no. 1, pp. 200–207, Jan. 2006.

[22] M. D. A. Thomas and P. B. Bamforth, “Modelling chloride diffusion in concrete Effect of fly ash and slag,” vol. 29, pp. 487–495, 1999.

[23] M. Liang, R. Huang, and H. Jheng, “REVISITED TO THE RELATIONSHIP BETWEEN THE FREE AND TOTAL,” vol. 18, no. 3, pp. 442–448, 2010.

[24] B. M. P. Mangat, “No Title,” *Mater. Struct.*, vol. 27, pp. 338–46, 1994.

[25] J. C. M. Maage, S. Helland, “Practical non-steady state chloride transport as a part of a model for predicting the initiation period,” *RILEM*, pp. 398–406.

[26] P. J. Tumidajski, “APPLICATION OF DANCKWERTS’ SOLUTION TO SIMULTANEOUS DIFFUSION AND CHEMICAL REACTION IN CONCRETE,” *Cem. Concr. Res.*, vol. 26, no. 5, pp. 697–700, 1996.

[27] P. V. Danckwerts, “Absorption by simultaneous diffusion and chemical reaction,” 1950, pp. 300–304.

[28] E. Bentz, DP; Garboczi, EJ; Lagergren, “Multi-scale microstructural modeling of concrete diffusivity: Identification of significant variables,” *Cem. Concr. AGGREGATES*, vol. 20, pp. 129–39.

[29] Y. Zeng, “Modeling of chloride diffusion in hetero-structured concretes by finite element method,” *Cem. Concr. Compos.*, vol. 29, no. 7, pp. 559–565, Aug. 2007.

[30] M. P. K., “Durability-Critical Issues for the Future,” *Concr. Int.*, vol. 19, no. 7, pp. 27–33, 1997.

[31] Y. Zhang, W. Sun, S. Chen, and F. Guo, “Two- and three-dimensional chloride ingress into fly ash concrete,” *J. Wuhan Univ. Technol. Sci. Ed.*, vol. 26, no. 5, pp. 978–982, Nov. 2011.

[32] Y.-S. Choi, J.-G. Kim, and K.-M. Lee, “Corrosion behavior of steel bar embedded in fly ash concrete,” *Corros. Sci.*, vol. 48, no. 7, pp. 1733–1745, Jul. 2006.

[33] C. 39 ASTM, “Standard Test Method for Compressive Strength of Cylindrical Concrete Specimens,” *Annu. B. ASTM Stand.*, vol. 4.02, 2005.

[34] M. Inc., “Wolfram Mathematica,” *Version 9.0*, 2013.

VITAE

Personal Information

Name : **MUHAMMAD UMAR KHAN**
Father's Name : ABDUL MALIK KHAN
Date of Birth : November 16, 1986
Nationality : Pakistani
Residential Address : House # G/1896, Tank # 3, Peshawari Para, Hyderabad, Pakistan
Email : umar_ce42@hotmail.com

Educational Qualification

S.No.	Name of Institution	Degree	Passing Year	CGPA
1.	King Fahd University of Petroleum and Minerals, Dhahran, Saudi Arabia	M.S. Civil Engineering (Structures)	December 2013	**4.0 / 4.0**
2.	Mehran University of Engineering and Technology, Hyderabad, Pakistan	B.E. Civil Engineering	March 2010	**3.90 / 4.0**

Professional Experience

1. **Employer : National Engineering Services Pakistan (NESPAK), Islamabad**

   Period : June 2010 - September 2011
   Position : Junior Engineer (Assistant Resident Engineer)
   Activities :Worked at the project of Federal Tribunal/ Courts Complex, G/11-1, Islamabad, Pakistan

Achievements:

- Hafiz-ul-Qur'an
- Secured "***TRIPLE HONORS***" **1 SLVER** and **2 GOLD** Medals in B.E.
- Achieved 1st Position in the Faculty (**Gold Medalist**)
- Maintained 1st Position throughout Graduation studies (**Best Graduate**)
- CGPA of **4.0/4.0** in MS

Membership

Registered Engineer with Pakistan Engineering Council